



**ROMANIAN ACADEMY**  
**SCHOOL OF ADVANCED STUDIES OF THE ROMANIAN**  
**ACADEMY INSTITUTE OF CHEMISTRY „Coriolan Drăgulescu”**

## **Ph.D. THESIS SUMMARY**

***HYBRID AND COMPOSITE NANOMATERIALS BASED  
ON PORPHYRIN DERIVATIVES  
WITH APPLICATIONS IN CORROSION INHIBITION AND  
DETECTION OF ANALYTES WITH MEDICAL AND  
TECHNICAL RELEVANCE***

PhD supervisor: CSI Dr. Ing. FĂGĂDAR-COSMA Eugenia

PhD student: EPURAN Camelia-Maria

**2024**

## TABLE OF CONTENTS

<b>LIST OF FIGURES</b> .....	7
<b>LIST OF TABLES</b> .....	17
<b>LIST OF ABBREVIATIONS</b> .....	18
<b>INTRODUCTION</b> .....	20
<b>References</b> .....	27
<b>CHAPTER I. Literature survey concerning the use of porphyrins as corrosion inhibitors and the use of their hybrid nanomaterials in the detection of analytes with medical and technical relevance</b> .....	30
1.1. General notions about porphyrins .....	30
1.2. Applications of porphyrin-bases and their platinum complexes in detection .....	32
1.3. Literature overview on the applications of organic-inorganic hybrid materials based on porphyrins and noble metals nanomaterials .....	33
1.4. Recent literature data concerning the application of porphyrins in corrosion inhibition...	35
1.5. References .....	38
<b>CHAPTER II. Apparatus used for the experiments</b> .....	50
2.1. UV-Vis spectrophotometer	50
2.2. Nuclear magnetic resonance spectrometer ( <sup>1</sup> H-NMR and <sup>13</sup> C-NMR) .....	50
2.3. FT/IR -4200 Spectrophotometer.....	50
2.4. Atomic force microscope .....	50
2.5. Fluorescence spectroscopy .....	51
2.6. X ray diffractometer .....	51
2.7. Thermogravimetric analysis equipment (TGA).....	51
2.8. Mass spectrometer .....	51
2.9. High performance liquid chromatography (HPLC) .....	52
2.10. References .....	52
<b>CHAPTER III. Obtaining of new porphyrin structures, metaloporphyrins and porphyrin trimers</b> .....	54
3.1. <i>Synthesis of the ester intermediate, 5-(methyl-4-benzoate)-10,15,20-tris-(4-methyl-phenyl)-porphyrin, starting from non-porphyrinic precursors and its physical-chemical characterization</i> .....	54

3.1.1. <sup>1</sup> H-NMR analysis of 5-(methyl-4-benzoate)-10,15,20-tris-(4-methyl-phenyl)-porphyrin .....	56
3.1.2. <sup>13</sup> C-NMR analysis of 5-(methyl-4-benzoate)-10,15,20-tris-(4-methyl-phenyl)-porphyrin .....	57
<b>3.2. Obtaining 5-(carboxy-4-benzoate)-10,15,20-tris-(4-methyl-phenyl)-porphyrin (5-COOH-3MPP) by hydrolysis of the ester derivative in basic medium .....</b>	<b>58</b>
3.2.1. Comparative analysis of the FT-IR spectra of the obtained compounds, before and after the hydrolysis reaction .....	59
3.2.2. <sup>1</sup> H-NMR analysis for 5-(carboxy-4-benzoate)-10,15,20-tris-(4-methyl-phenyl)-porphyrin .....	59
3.2.3. UV-Vis spectrometric study of 5-(carboxy-4-benzoate)-10,15,20-tris-(4-methyl-phenyl)-porphyrin .....	61
3.2.3.1. Protonation and aggregation phenomena in acidic or basic media revealed by UV-Vis spectrometry for 5-(carboxy-4-benzoate)-10,15,20-tris-(4-methyl-phenyl)-porphyrin.....	61
3.2.3.1.1. Study of the behavior in acidic medium .....	61
3.2.3.1.2. Study of the optical behaviour in basic medium .....	62
<b>3.3. Obtaining and characterization of 5,10-(4-carboxy-phenyl)-15,20-(4-phenoxy-phenyl)-porphyrin (cis) .....</b>	<b>64</b>
3.3.1. <sup>1</sup> H-NMR analysis for 5,10-(4-carboxy-phenyl)-15,20-(4-phenoxy-phenyl)-porphyrin. The influence of the symmetry of the molecule .....	67
3.3.2. Physical-chemical characterization of 5,10-(4-carboxy-phenyl)-15,20-(4-phenoxy-phenyl)-porphyrin by UV-Vis spectroscopy .....	68
3.3.3. FT-IR characteristic aspects regarding 5,10-(4-carboxy-phenyl)-15,20-(4-phenoxy-phenyl)-porphyrin.....	68
3.3.4. Morphological particularities evidenced by atomic force microscopy for 5,10-(4-carboxy-phenyl)-15,20-(4-phenoxy-phenyl)-porphyrin .....	69
<b>3.4. Synthesis and characterization of a new metaloporphyrin structure, Pt(II)-5-(4-carboxy-phenyl)-10,15,20-tris-(4-phenoxy-phenyl)-porphyrin (Pt(II)-COOH-TPOPP).....</b>	<b>70</b>
3.4.1. UV-Vis monitoring during the obtaining of Pt(II)-5-(4-carboxy-phenyl)-10,15,20-tris-(4-phenoxy-phenyl)-porphyrin .....	72
3.4.2. <sup>1</sup> H-NMR interpretation for Pt(II)-COOH-TPOPP .....	74
3.4.3. <sup>13</sup> C-NMR analysis for the obtained Pt-metalated porphyrin .....	75
3.4.4. Comparative FT-IR analysis of the compounds, before and after the metalation reaction .....	76
3.4.5. Thermal stability. Thermogravimetric analysis for COOH-TPOPP and Pt(II)-COOH-TPOPP .....	77
3.4.6. AFM investigation of morphological characteristics for Pt(II)-COOH-TPOPP .....	79

<b>3.5. Obtaining of a new hetero-trimer porphyrin structure by interaction between a porphyrin-base and a Pt(II)- metaloporphyrin .....</b>	80
3.5.1. Synthesis and characterization of the trimer obtained from (5,10,15,20-tetra-(4 sulfonato-phenyl)-pophyrin and Pt(II)-5,10,15,20-tetra-(4-allyloxy-phenyl)-porphyrin ....	81
3.5.1.1. UV-Vis spectroscopic monitorization during the formation of the (Pt-aliloxi-PP-TSPP) hetero-trimer .....	82
3.5.1.2. <sup>1</sup> H-NMR evidence for the formation of Pt-aliloxiPP-TSPP hetero-trimer .....	84
3.5.1.3. Comparative FT-IR analysis of the individual porphyrins and the newly formed hetero-trimer .....	86
3.5.1.4. Chapter conclusions .....	88
3.5.1.5. References.....	88
<b>CHAPTER IV. Applications of porphyrins in formulation of sensors. Potentiometric sensor for the detection of citrate ion, based on (Pt(II)-COOH-TPOPP) as ionophore .....</b>	97
4.1. The importance of citrate ion detection .....	98
4.2. Obtaining of sensitive membranes used in potentiometric detection.....	98
4.2.1. Preparation of the sensitive electrode membranes and performing the measurements.....	98
4.3. Potentiometric detection of citrate ion using Pt(II)-COOH-TPOPP as ionophore .....	100
4.4. Proposed mechanism for the citrate ion recognition .....	103
4.5. Analytical applications of Sensor 1 .....	104
4.6. Conclusions .....	105
4.7. References .....	107
<b>CHAPTER V. Fluorimetric sensor for the detection of toluidine blue using (Pt-aliloxiPP-TSPP) porphyrin hetero-trimer as sensitive material .....</b>	110
5.1. The importance of touidine blue detection .....	115
5.2. Fluorimetric toluidine blue detection using Pt-aliloxiPP-TSPP hetero-trimer as sensitive material .....	115
5.2.1. Method of working .....	115
5.3. Interferent study in the fluorimetric detection of toluidine blue using Pt-aliloxiPP-TSPP hetero-trimer as sensitive material.....	120
5.3.1. Method for studiing of interference efects from different species.....	120
5.4. Morphological analysis of the sensitive material before and after toluidine blue recognition .....	121
5.5. Comparative analysis of FT-IR spectra recorded for Pt-aliloxiPP-TSPP hetero-trimer before and after toluidine blue detection .....	123

5.6. Proposed mechanism for the recognition of toluidine blue by the Pt-aliloxiPP-TSPP hetero-trimer.....	124
5.7. Conclusions .....	125
5.8. References .....	126
<b>CHAPTER VI. Multifunctional composite materials based on porphyrins substituted with carboxylic moieties, k-carrageenan and nano-Au with applications in the detection/capture of CO<sub>2</sub> and the detection of Mn<sup>2+</sup> ions .....</b>	131
6.1. Importance of the CO <sub>2</sub> detection/capture .....	133
6.2. Obtaining composite materials for the detection/capture CO <sub>2</sub> in aqueous media.....	134
6.2.1. Obtaining the (5-COOH-3MPP)-k-carrageenan composite material .....	134
6.2.2. Testing the sensibility of the (5-COOH-3MPP)-k-carrageenan composite to CO <sub>2</sub> . Monitoring by UV-Vis spectroscopy.....	135
6.2.3. Testing the capacity of the (5-COOH-3MPP)-k-carrageenan composite to capture CO <sub>2</sub> by fluorescence emission measurements .....	137
6.2.4. AFM analysis of the (5-COOH-3MPP)-k-carrageenan composite material before and after exposure to CO <sub>2</sub> .....	139
6.3. (5-COOH-3MPP)-k-carrageenan composite material functionalized with AuNPs. Study of its capacity to detect Mn <sup>2+</sup> cations .....	141
6.3.1. Importance of the monitorization of (Mn <sup>2+</sup> ) .....	141
6.3.2. Method for obtaining of (5-COOH-3MPP)-k-carrageenan-AuNPs hybrid material.....	142
6.3.3. UV-Vis Spectrophotometric Mn <sup>2+</sup> ions detection using (5-COOH-3MPP)-k-carrageenan-AuNPs hybrid material as sensitive material.	145
6.3.4. Morphological changes in the (5-COOH-3MPP)-k-carrageenan-AuNPs hybrid material before and after the detection of Mn <sup>2+</sup> evidenced by AFM .....	146
6.3.5. Interference studies .....	147
6.4. Conclusions .....	149
6.5. References .....	149
<b>CHAPTER VII. Hybrid materials based on porphyrins and CuNPs, PtNPs and Pt@CuNPs respectively. Applications in the optical detection of uric acid .....</b>	155
7.1. Importance of uric acid detection .....	156
7.2. Obtaining of the necessary materials .....	157
7.2.1. Synthesis of 5,10,15,20-tetrakis-(4-amino-phenyl)-porphyrin (TAmPP) .....	157
7.2.2. Obtaining and physical-chemical characterization of metal nanoparticles: (CuNPs), (PtNPs) and of copper core surrounded by a platinum shell (Pt@CuNPs).....	157
7.2.2.1. Synthesis of colloidal platinum.....	157

7.2.2.2. Synthesis of colloidal copper .....	158
7.2.2.3. Obtaining of mixed nanoparticles with Cu core and Pt shell Pt@CuNPs) .....	159
7.2.3. X-Ray diffraction (XRD) characterization of the CuNPs, PtNPs and platinum covered copper core nanoparticles (Pt@CuNPs) .....	160
7.2.4. Emission-scanning electron microscopy (SEM EDAX) characterization of the CuNPs, PtNPs and (Pt@CuNPs) nanoparticles .....	161
7.3. Hybrid materials based on 5,10,15,20-tetrakis-(4-amino-phenyl)-porphyrin (TAmPP) and CuNPs, PtNPs and Cu@PtNPs respectively .....	162
7.3.1. Method for obtaining of the hybrid material between TAmPP and PtNPs .....	162
7.3.2. Method for obtaining of the hybrid material between TAmPP and CuNPs.....	163
7.3.3. Method for obtaining of the hybrid material between TAmPP and Pt@CuNPs ...	167
7.4. Detection of uric acid by 5,10,15,20-tetrakis-(4-amino-phenyl)-porphyrin (TAmPP) or the hybrid materials based on (TAmPP) and CuNPs, PtNPs or Pt@CuNPs respectively.....	168
7.4.1. Detection of uric acid using acidified TAmPP solution in DMSO .....	168
7.4.1.1. Proposed mechanism for the detection of uric acid by TAmPP in solution.....	169
7.4.1.2. Interference effect study .....	170
7.4.2. Detection of uric acid with TAmPP- CuNPs hybrid material .....	171
7.4.2.1. Interference effect study.....	173
7.4.3. Detection of uric acid with TAmPP-PtNPs hybrid material .....	174
7.4.3.1. Study of interferent species effects .....	175
7.4.4. Detection of uric acid using TAmPP- Pt@CuNPs hybrid as sensitive material .....	176
7.4.4.1. Study of potential interferent species .....	178
7.5. Conclusions .....	179
7.6. References .....	180
<b>CHAPTER VIII. Hybrid materials obtained between porphyrins and pseudo-binary oxides. New composites for corrosion inhibition .....</b>	<b>183</b>
8.1. Corrosion inhibitors based on porphyrins for carbon-steel protection. General technical specifications .....	183
8.2. Carbon-steel protection using as corrosion inhibitors two porphyrins, each bearing two COOH functional groups, differently positioned in <i>cis</i> and <i>trans</i> .....	184
8.2.1. Obtaining and characterization of the porphyrins and pseudo-binary oxides That form the protective thin films .....	185
8.2.1.1. <i>Short presentation of obtaining and characterization of the two A<sub>2</sub>B<sub>2</sub>-type porphyrins used in corrosion inhibition studies .....</i>	185

8.2.1.2. Short presentation for obtaining and characterization of $MnTa_2O_6$ pseudo-binary oxide.....	186
8.2.2. Drop-casting deposition and characterization of protective films consisting in alternative porphyrin/oxide sandwich type layers .....	187
8.2.3. Electrochemical corrosion tests .....	188
8.2.4. Morphological study of protective thin films obtained by the drop-casting method .....	190
8.3. Obtaining and characterization of protective layers obtained by MAPLE and PLD depositions, using as corrosion inhibitors porphyrins with one COOH or one ester functional group in association with $MnTa_2O_6$ pseudo-binary oxide .....	196
8.3.1. Obtaining and characterization of sandwich-type porphyrin-oxide protective layers deposited by coupled PLD and MAPLE techniques .....	198
8.3.2. Electrochemical corrosion tests .....	199
8.3.3. Morphological analysis of the thin films obtained by combined MAPLE and PLD laser methods.....	202
8.4. Conclusions of the chapter .....	207
8.5. References .....	209
<b>General conclusions and original cotributions .....</b>	<b>212</b>
<b>Papers published related to the defened doctoral thesis .....</b>	<b>220</b>

## Introduction

The interest in the chemistry of porphyrins is continuously growing due to their multifunctional character. This class of compounds is particularly versatile, being involved in a multitude of applications, such as: the development of optical sensors [1,2], fluorescence [3,4], potentiometric [5] and also in expanding the range of corrosion inhibitors [6], of catalysts and photosensitive substances useful in medicine, optical detection and medical imaging [7,8].

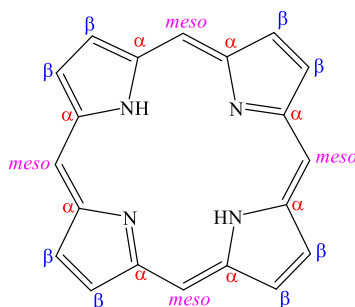


**Figure 1.** Molecular structure of porphyrin-base.

Porphyrins exhibit thermal and chemical stability and the optical and electronic properties of porphyrins can be modified by the function of grafted substituents on the macrocycle [9].

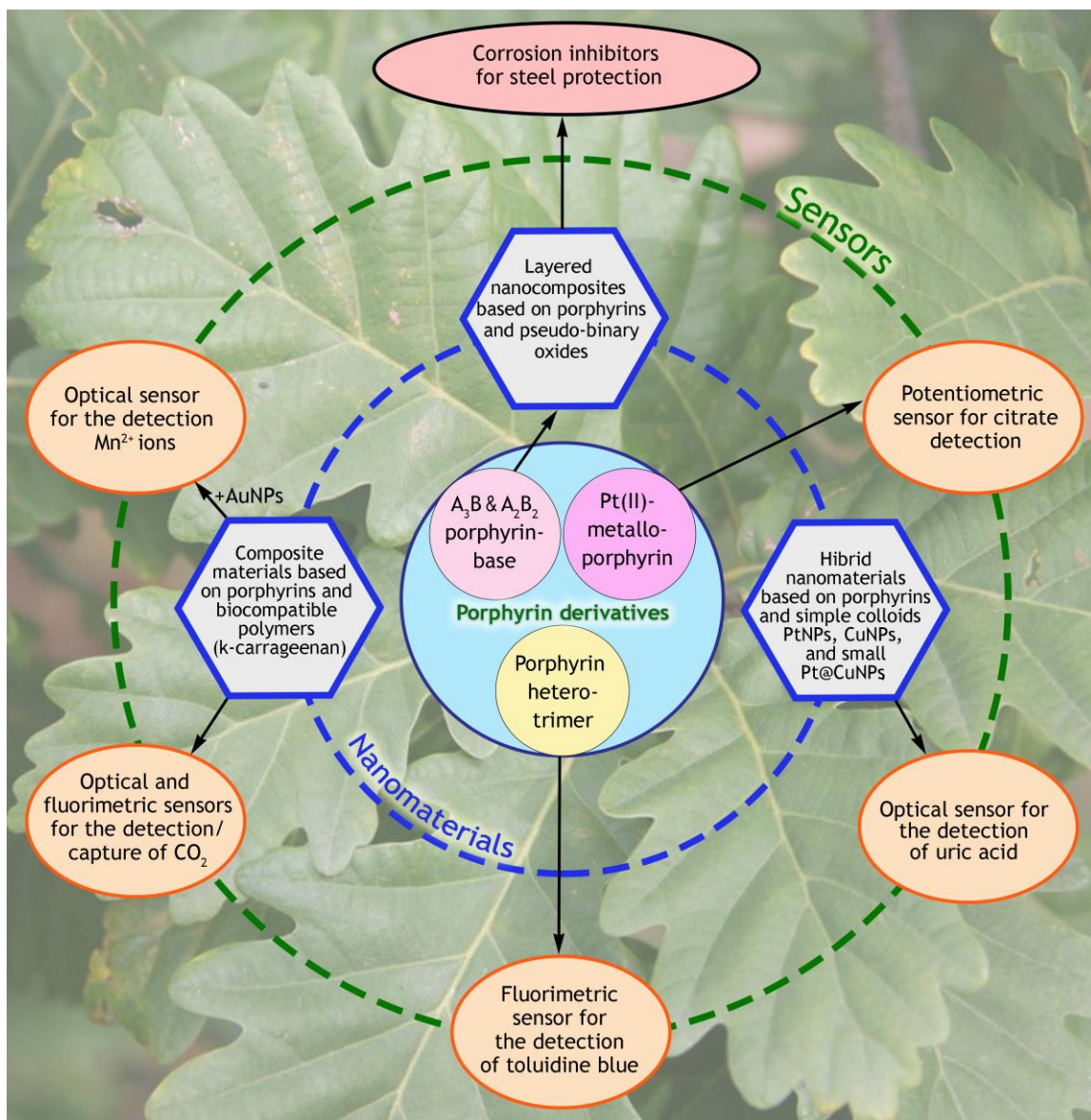
A highly exploitable feature of porphyrins is their ability to be used as building blocks in the formation of supramolecular aggregates, because they possess the capacity of both self-assembly and self-organization [10].

In the case of this doctoral thesis, it was proposed to obtain new structures of *meso*-substituted porphyrins, both unmetallated and metallated because the optoelectronic properties and detection sensitivity can be improved both by introducing a carefully selected metal ion inside the porphyrinic macrocycle, and by grafting peripheral substituents that change the hydrophilic-hydrophobic balance of the newly created tetrapyrrole structures [10]. Since *meso*-substituted porphyrins are not found in nature, their synthesis and applications in various fields are of great interest for research. Original aspects both from the point of view of porphyrin chemistry and application potential are brought by the hetero-trimeric structures, designed so that the constituent porphyrin molecules potentiate the desired properties.

Obtaining new hybrid nanomaterials based on porphyrins, made in partnership with nanoparticles of different metals (CuNPs, PtNPs, Pt@CuNPs, AuNPs) and incorporated in a non-toxic organic polymer (k-carrageenan) or by combining with pseudo-binary oxides represents basis for the formulation of new sensors or the creation of new corrosion inhibitors.

The original aspects of the doctoral thesis are presented in the Scheme 1.





**Scheme 1.** The main innovative aspects and obtained results of the doctoral thesis.

### **Research objectives:**

*The main and specific objectives of the doctoral thesis are intended to increase the level of knowledge in the chemistry of porphyrins and to identify technically and medically relevant applications:*

- ❖ *The design, synthesis and complete physical-chemical characterization of novel structures of porphyrin-bases and metalloporphyrins, as well as hetero-porphyrin trimers*

- Obtaining new structure of mixed-substituted A<sub>3</sub>B porphyrins-bases: *5-(methyl-4-benzoate)-10,15,20-tris-(4-methyl-phenyl)-porphyrin* and *5-(4-carboxy-phenyl)-10,15,20-tris-(4-methyl-phenyl)-porphyrin* as well as A<sub>2</sub>B<sub>2</sub>, *5,10-(4-carboxy-phenyl)-15,20-(4-phenoxy-phenyl)-porphyrin (cis)*;
- Obtaining metalloporphyrin: *Pt(II)-carboxy-phenyl-tris-(phenoxy-phenyl)-porphyrin*
- *The new hetero-trimeric structure (Pt-allyloxy-PP-TSPP)*, obtained by combining a water-soluble porphyrin (5,10,15,20-tetra-(4-sulfonato-phenyl)-porphyrin) and a metalloporphyrin (Pt(II)-5,10,15,20-tetra-(4-allyloxy-phenyl)-porphyrin);
- ❖ *Obtaining hybrid nanomaterials based on porphyrins, realized in partnership with copper nanoparticles (CuNPs), platinum nanoparticles (PtNPs) and mixed nanoparticles with Cu core and Pt shell (Pt@CuNPs)*
- ❖ *The realization of multifunctional composite materials based on biocompatible organic polymer (k-carrageenan) and a functionalized porphyrin with a COOH group: 5-(4-carboxy-phenyl)-10,15,20-tris-(4-methyl-phenyl)- porphyrin (5-COOH-3MPP).*
  - Functionalization with gold nanoparticles (AuNPs) of the hybrid material (5-COOH-3MPP-k-carrageenan) to enhance the optical properties.
- ❖ *Complete physical-chemical characterization by structural, optical and morphological methods of the newly obtained structures and materials.*
  - Performing TLC, HPLC, FT-IR, UV-Vis, fluorescence, <sup>1</sup>H-NMR and <sup>13</sup>C-NMR, mass MS (ESI+), AFM microscopy studies.
- ❖ *Original corrosion inhibitor systems based on alternative thin layers formed by porphyrins and pseudobinary oxides and their use for steel corrosion inhibition.*
  - The development of appropriate materials for the formation of thin films by *drop-casting* and laser techniques (MAPLE and PLD) that exhibit steel corrosion inhibition properties;
  - Study by atomic force microscopy (AFM) of the specific self-aggregation properties of porphyrins (5-(4-carboxy-phenyl)-10,15,20-tris(4-methyl-phenyl)-porphyrin; 5,10-(4-carboxy-phenyl)-15,20-(4-phenoxy-phenyl)-porphyrin; 5,15-(4-carboxy-phenyl)-10,20-phenyl-porphyrin), as well as on the capacity of some pseudo-binary oxides (MnTa<sub>2</sub>O<sub>6</sub>) to uniformly cover the steel surface, producing physical barriers against the action of aggressive environments;

- Study of the effects induced by the number and position of the carboxyl groups grafted on the porphyrinic heterocycle on the corrosion inhibition efficiency, performed by electrochemical methods;
  - Identifying and validating the mechanisms of corrosion inhibition.
- ❖ *Applications of new porphyrin structures and their hybrid materials for obtaining new, more efficient optical, fluorometric and potentiometric sensors*
- Creation of a fluorimetric sensor based on the Pt-allyloxyPP-TSPP hetero-trimer for the detection of toluidine blue - a scientific priority;
  - *Ion-selective membrane sensor* based on *Pt(II)-5-(4-carboxyphenyl)-10,15,20-tris-(4-phenoxy-phenyl)-porphyrin* used as ionophore to *detect citrate anion by potentiometric method*;
  - *Optical and fluorimetric sensor* based on a composite material obtained between (5-COOH-3MPP) and k-carrageenan for the *detection/capture of CO<sub>2</sub>, the first reported to work efficiently under normal conditions*;
  - *Optical sensor based on three-component nanomaterial porphyrin-k-carrageenan-AuNPs to recognize and quantify Mn<sup>2+</sup> ions*;
  - *Sensors on complementary concentration domains for the detection of uric acid using inorganic-organic hybrid nanomaterials* obtained by complexing a symmetrical amino-substituted porphyrin with simple or mixed colloidal metallic nanoparticles: PtNPs, CuNPs or Pt@CuNPs.

## **Original experimental results and discussion**

Chapters 3-8 of the doctoral thesis present the experimental studies carried out in order to obtain and fully characterize the new porphyrinic derivatives as well as their applications and their hybrid nanomaterials in the creation of new sensors for the detection of citrate ion (Chapter IV), toluidine blue (Chapter V) Mn<sup>2+</sup> ion (Chapter VI), uric acid (Chapter VII). Of great impact and aligned with current trends is the creation of a porphyrin-k-carrageenan composite material capable of recognizing, detecting and capturing CO<sub>2</sub> in normal atmospheric conditions (Chapter VI). The development of materials capable to form thin films, deposited on the surface of different steels by drop-

casting and laser techniques (MAPLE and PLD), which demonstrated steel corrosion inhibition properties are detailed in Chapter VIII.

Chapter 3 presents the preparation of new structures of mixed substituted  $A_3B$  porphyrins: 5-(methyl-4-benzoate)-10,15,20-tris-(4-methyl-phenyl)-porphyrin which was subsequently hydrolyzed to 5-(4-carboxy-phenyl)-10,15,20-tris-(4-methyl-phenyl)-porphyrin and  $A_2B_2$ , 5,10-(4-carboxy-phenyl)-15,20-(4-phenoxy-phenyl)-porphyrins (cis) by multicomponent Adler-Longo type reactions between two differently substituted benzaldehydes and pyrrole. A new hetero-trimer structure and a new Pt(II)-metalloporphyrin structure were also reported in this chapter.

The compounds obtained (Figure 2, a-c) were purified and fully characterized by the following physico-chemical techniques: TLC chromatography and by the HPLC technique, mass spectroscopy MS (ESI+),  $^1\text{H-NMR}$ ,  $^{13}\text{C-NMR}$ , FT-IR, UV-Vis.

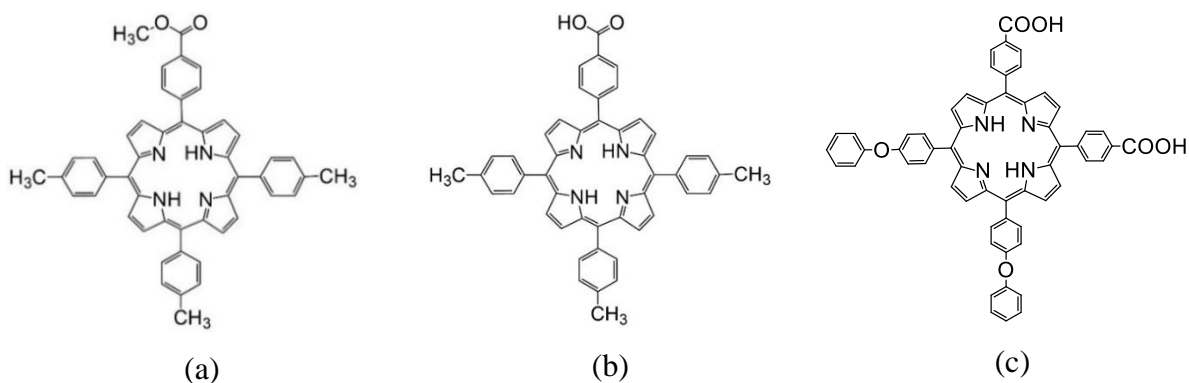


**Figure 2.** Chemical structures of 5-(4-methyl-benzoate)-10,15,20-tris-(4-methyl-phenyl)-porphyrin (a); 5-(4-carboxy-phenyl)-10,15,20-tris-(4-methyl-phenyl)-porphyrin (b) and 5,10-(4-carboxy-phenyl)-15,20-(4-phenoxy-phenyl)-porphyrin (c).

As can be seen in Figure 2, a pair of porphyrins was obtained: the methyl ester (Figure 2 a) respectively the mono-substituted porphyrin with the functional group  $-\text{COOH}$  (Figure 2 b), whose  $^1\text{H-NMR}$  spectra are comparatively discussed below.

The  $^1\text{H-NMR}$  spectrum of compound 5-(4-methyl-benzoate)-10,15,20-tris-(4-methyl-phenyl)-porphyrin (Figure 3) completely justify the structure. The unshielded  $\beta$ -pyrrolic protons resonate in the range 8.91 - 8.79 ppm; the *ortho*-phenyl protons and the corresponding *meta*-phenyl protons from methyl-benzoate substituent appear as two doublets in the 8.47 - 8.45 ppm interval and respectively as between 8.34 and 8.32 ppm; the two doublets located at 8.13 - 8.11 ppm

interval and between 7.59 to 7.57 ppm range are assigned to *ortho*-phenyl protons and respectively *meta*-phenyl protons from the tolyl group; the equivalent aliphatic protons of -OCH<sub>3</sub> substituent resonate as singlet signal at 4.13 ppm; the protons belonging to the -CH<sub>3</sub> groups are also equivalent and appear as singlet at 2.73 ppm. The internal -NH protons are distinctively placed at -2.74 ppm, due to intense shielding, caused by the second generated magnetic field.

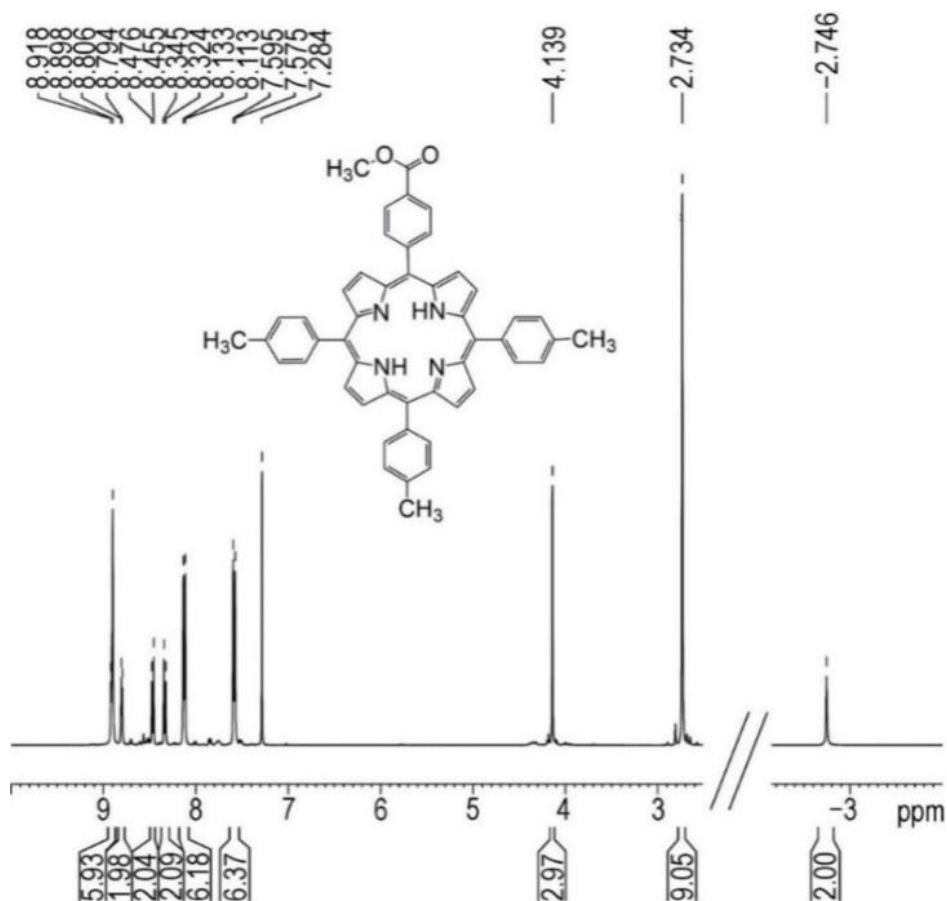


**Figure 3.** <sup>1</sup>H-NMR spectrum of 5-(4-methyl-benzoate)-10,15,20-tris-(4-methyl-phenyl)-porphyrin in CDCl<sub>3</sub>.

The <sup>1</sup>H-NMR spectrum of the compound 5-(4-carboxy-phenyl)-10,15,20-tetra-(4-methyl-phenyl)-porphyrin (Figure 4) presents the characteristic signals confirming the structure of the hydrolyzed compound. It can be observed that the singlet signal specific for the three protons of the -OCH<sub>3</sub> group found in the ester at 4.13 ppm is no longer present, fact that confirms the hydrolysis of the ester to carboxylic acid. The six equivalent β-pyrrolic protons, which are unshielded, resonate as a doublet in the range 8.89-8.78 ppm and the other two equivalent β-pyrrolic protons in the A<sub>3</sub>B structure presented a singlet signal at 8.712 ppm; *ortho*-phenyl protons

from benzoic acid showed signal in the range 8.493-8.479 ppm and the *meta*-phenyl protons from benzoic acid stand out in the range 8.357-8.377 ppm; *ortho*-phenyl protons from the tolyl group give a signal in the range 8.119-8.091 ppm; the *meta*-phenyl protons of the tolyl group is highlight in the range 7.574-7.555 ppm. Protons of groups – CH<sub>3</sub> show a chemical displacement at 2.712 ppm, as a singlet signal, for the 9 equivalent protons; internal protons from the porphyrin cycle – NH give singlet signal at –2.771 ppm because they are strongly shielded.

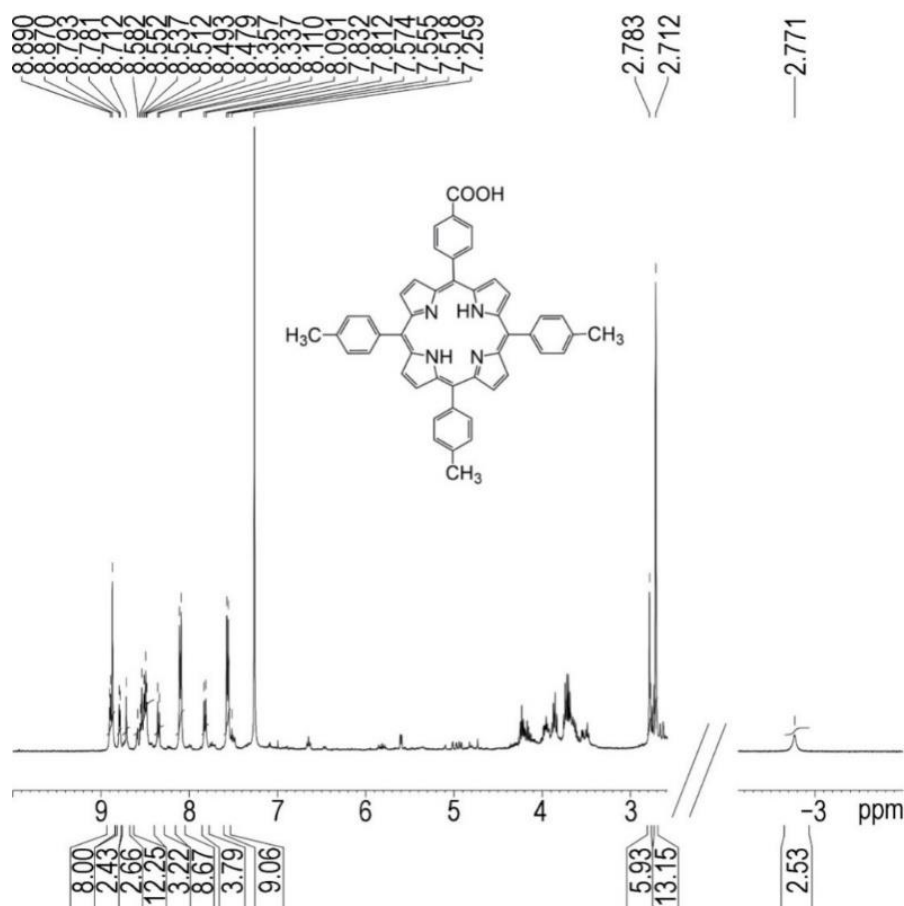


**Figure 4.** <sup>1</sup>H-NMR spectrum in CDCl<sub>3</sub> of 5-(4-carboxy-phenyl) -10,15,20-tris-(4-methyl-phenyl)-porphyrin.

The metalloporphyrin Pt(II)-carboxy-phenyl-tris-(phenoxy-phenyl)-porphyrin was obtained by the direct metalation reaction using bis(benzonitrile)platinum(II) chloride (PtCl<sub>2</sub>(PhCN)<sub>2</sub>) in excess (Figure 5). The structure of the obtained compound was confirmed by nuclear magnetic resonance spectra <sup>1</sup>H-NMR, <sup>13</sup>C-NMR and by the compared vibrational-rotational FT-IR spectra.



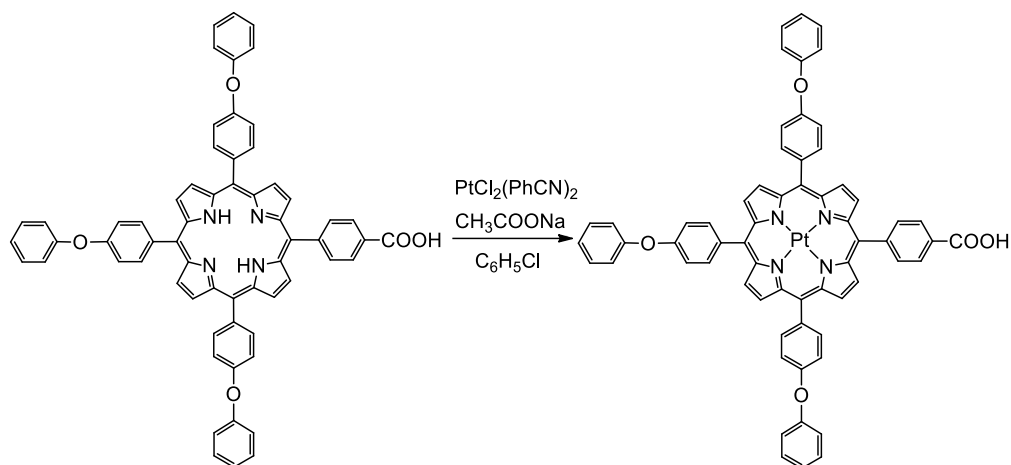


**Figure 5.** Reaction to obtain Pt(II)-carboxy-phenyl-tris-(phenoxy-phenyl)-porphyrin (Pt(II)-COOH-TPOPP).

The generation of metalloporphyrin was monitored by UV-Vis spectroscopy (Figure 6). During metalation, the Soret band suffer both a hypsochromic effect and a blue shifting effect from 224 nm to 406 nm. It can be noticed that the number of Q bands also decreases.

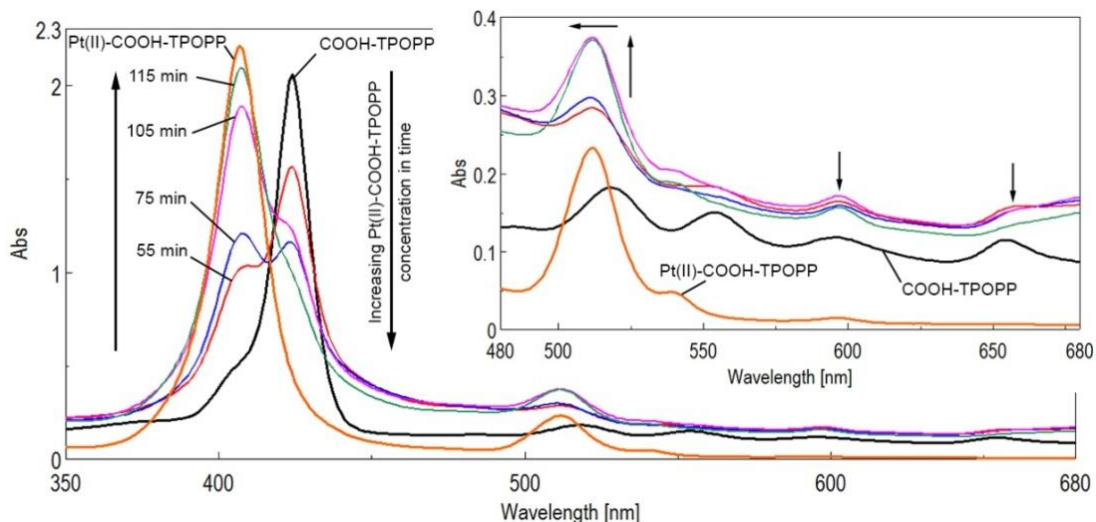


**Figure 6.** UV-Vis monitoring of the metalation process of a COOH-TPOPP during the preparation of Pt(II)-COOH-TPOPP. Detail of the Q bands for the intermediate and final products during the reaction.

The FT-IR spectrum (Figure 7), confirms the full metalation of the free-base porphyrin. In the spectrum of Pt-COOH-TPOPP, the peak assigned to internal N-H bonds vibration, located at  $3316\text{ cm}^{-1}$  in the porphyrin base spectrum, does no longer exists. Comparing the FT-IR spectra of the two compounds, the COOH-TPOPP porphyrin [11] and its Pt-metalloporphyrin, evidences

some common features [12-17]:  $2897\text{-}2916\text{ cm}^{-1}$  ( $\nu_{\text{C-H}}$ ),  $1677\text{-}1684\text{ cm}^{-1}$  ( $\nu_{\text{COO}_{\text{as}}}$ ),  $1595\text{-}1592\text{ cm}^{-1}$  ( $\nu_{\text{C=C}}$ ),  $1481\text{ cm}^{-1}$  ( $\nu_{\text{C-O-C}}$  and  $\nu_{\text{C=N}}$ ),  $1234\text{ cm}^{-1}$  ( $\nu$  and  $\delta_{\text{Ar}}$  C–O–C),  $1163\text{ cm}^{-1}$  ( $\delta_{\text{N-H}}$ ),  $1105\text{-}1113\text{ cm}^{-1}$  ( $\nu_{\text{C-O}}$ ),  $793\text{ cm}^{-1}$  ( $\gamma_{\text{C-H}}$  pyrrole).

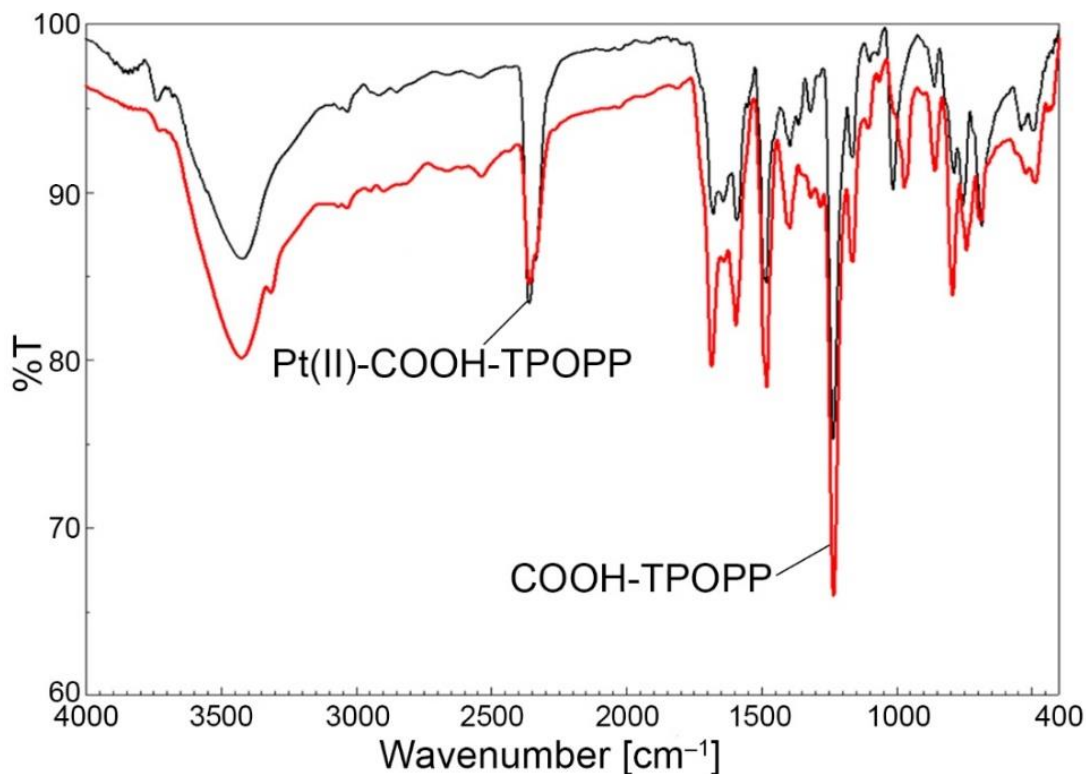


**Figure 7.** Overlapped FT-IR spectra of COOH-TPOPP and Pt(II)-COOH-TPOPP in KBr pellets.

The  $^1\text{H-NMR}$  spectrum of Pt(II)-COOH-TPOPP is represented in Figure 8 and has the main signals, as follows: 8.84–8.83 ppm (d, 8H,  $\beta$ -pyrrole), 8.11–8.09 ppm (d, 8H, 2,6-phenyl), 7.81–7.79 ppm (d, 8H, 3,5-phenyl), 7.75–7.72 ppm (t, 3H, 4\*-phenyl), 7.58–7.55 ppm (t, 6H, 3\*,5\*-phenyl), 7.36–7.34 ppm (d, 6H, 2\*,6\*-phenyl).



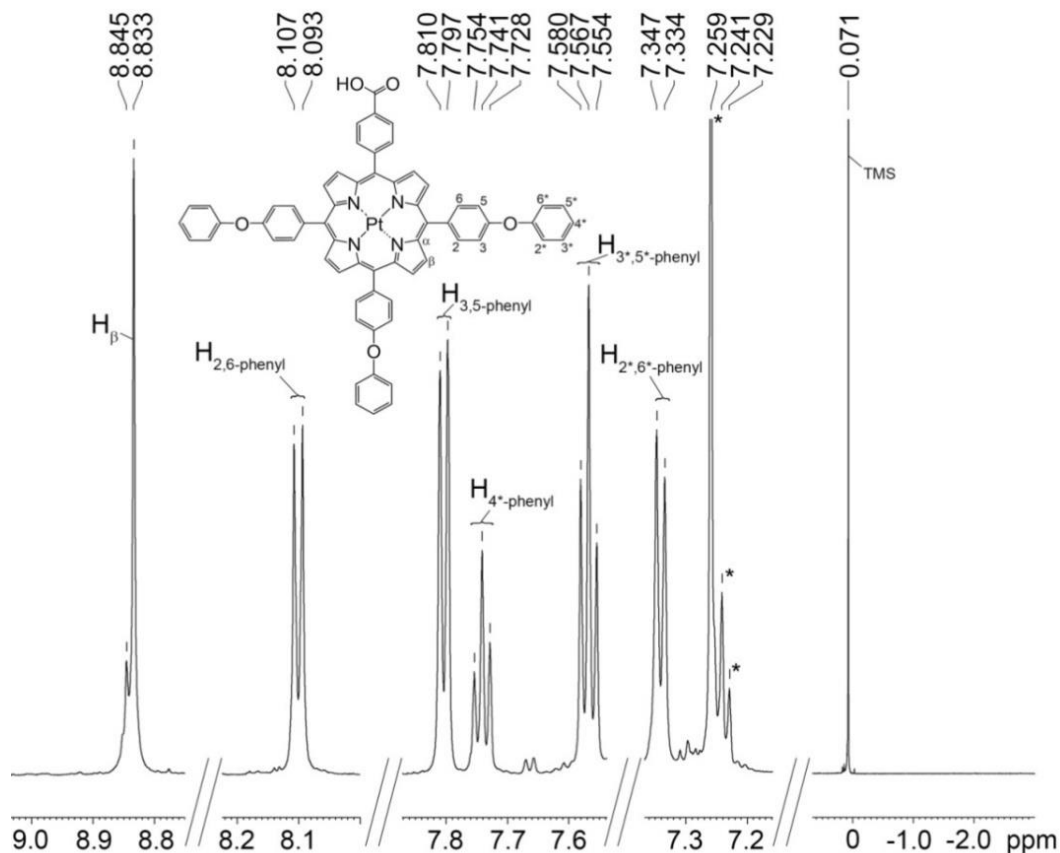


**Figure 8.**  $^1\text{H}$ -NMR magnetic resonance spectrum of Pt(II)-COOH-TPOPP in  $\text{CDCl}_3$ .

From the need to make new sensitive substances, with appropriate structures, conformation and interaction capacity, for the detection of anions/cations, the design for a new type of porphyrin hetero-trimer was thought by the direct combination of two different porphyrin molecules [18,19].

*The hetero-trimer (Pt-allyloxy-PP-TSPP)* combined the properties of a metallated porphyrin, Pt(II)-5,10,15,20-tetrakis-(4-allyloxyphenyl)-porphyrin (Pt-allyloxyPP), and of two molecules of a water-soluble porphyrin, 5,10,15,20-tetrakis(4-sulfonatophenyl)-porphyrin (TSPP). TSPP molecules were axially bonded via oxygen atoms to the platinum atom in the centre of Pt-allyloxyPP molecule. *Pt-allyloxy-PP-TSPP* was completely characterized by  $^1\text{H}$ -NMR, UV-Vis, FT-IR spectroscopy to prove the structure and by fluorescence.

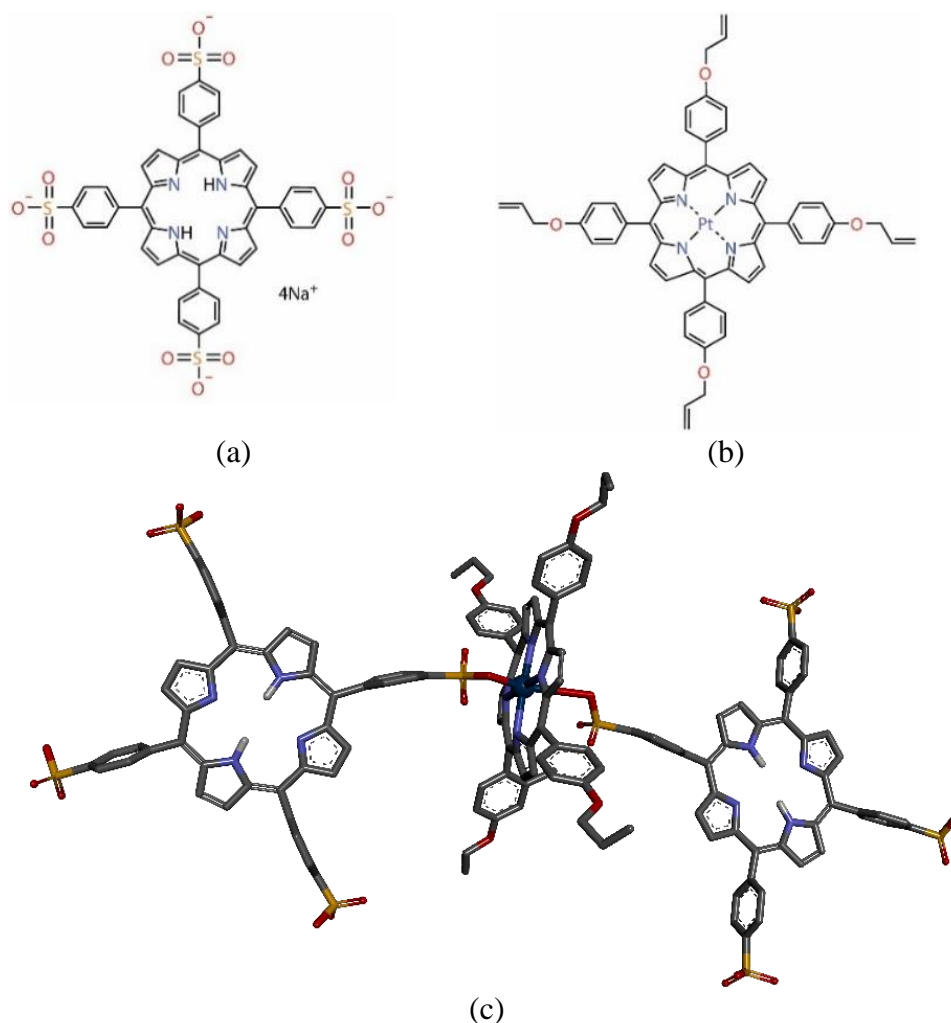


**Figure 9.** Chemical structures for (a) Pt(II)-5,10,15,20-tetrakis-(4-allyloxyphenyl)-porphyrin (Pt-allyloxyPP); (b) 5,10,15,20-tetrakis(4-sulfonatophenyl)-porphyrin (TSPP); and (c) Proposed structure of the Pt-allyloxyPP-TSPP heterotrimer, optimized with PyMOLMolecular Graphics System.

A comparison of the FT-IR spectra of the Pt-allyloxyPP-TSPP heterotrimer (Figure 10) with the initial porphyrins, put into evidence the new peaks located at  $490\text{ cm}^{-1}$  and  $549.5\text{ cm}^{-1}$  (blue circles in Figure 10) assigned to the newly created Pt–O bond and representing its bending vibration.

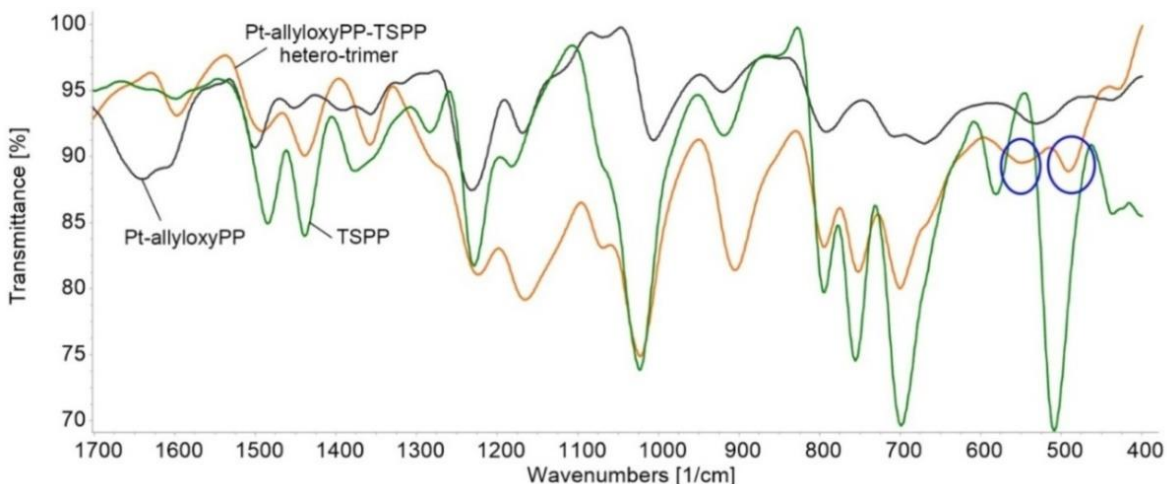


**Figure 10.** Overlapped FT-IR spectra for TSPP, Pt-allyloxyPP, and the Pt-allyloxyPP-TSPP hetero-trimer, as KBr pellets. The new generated bonds are marked in blue circles.

**Chapters 4 and 5 present applications of the new porphyrin structures to obtain new, more efficient, fluorimetric and potentiometric sensors.**

*In chapter 5, it is reported the priority in development of a fluorimetric sensor for toluidine blue* exploiting the exceptional emission properties of the *hetero-trimer Pt-allyloxyPP-TSPP*, due to the synergistic effect achieved between the two porphyrin components of the new system.

**The following applications are mentioned as notable results:**

The fluorimetric sensor, based on hetero-trimer was capable to detect toluidine blue in the concentration domain of  $1.9 \times 10^{-6} - 6.39 \times 10^{-5}$  M, with an excellent sensitivity and precision, due to enhanced emission properties and multiple acidic binding sites.

The domain is biologically relevant for the remained toxicity after monitoring cells by imagistic methods.

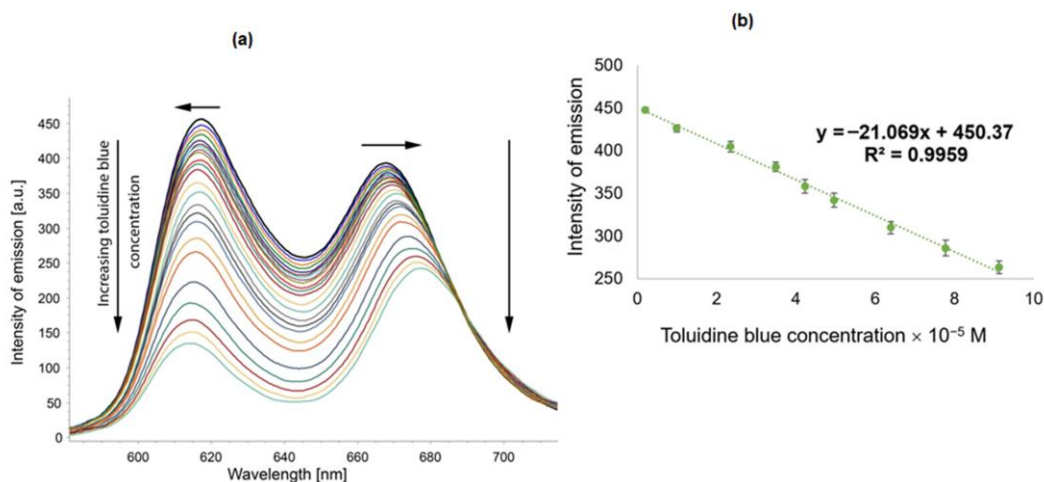


**Figure 11.** Emission spectra recorded during the addition of toluidine blue to the acidified solution (pH= 2) of Pt-allyloxyPP-TSPP hetero-trimer in DMSO (a) and the linear dependence between the emission intensity measured at 617 nm of the hetero-trimer in DMSO and toluidine blue concentration.

Colorimetric changes (yellow to greenish blue) of the Pt-allyloxy-TSPP hetero-trimer solution before and after contact to TB in visible (Figure 12 a) and, respectively, under ultraviolet excitation (Figure 12 b) were notified, so that a new way is opened for colorimetric detection.

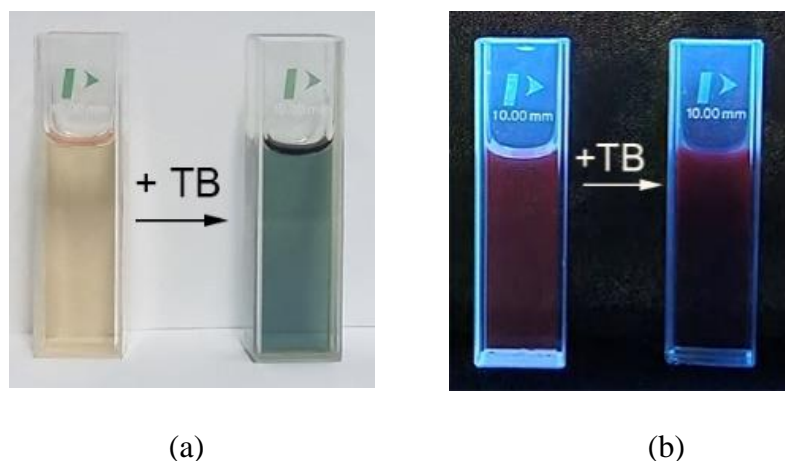


**Figure 12.** Photographic images of the Pt-allyloxy-TSPP trimer before and after exposure to TB, (a) in visible light and (b) under ultraviolet irradiation at 254 nm.

The mechanism for TB detection (Figure 13) was elucidated after using the program PyMOL molecular graphics system and based on appropriated distances and spatial geometries. Three main interactions explain the mechanism of detection: Columbian forces (orange bonds); hydrogen bonds (green bonds) and  $\pi$ - $\pi$  interaction (yellow bonds).

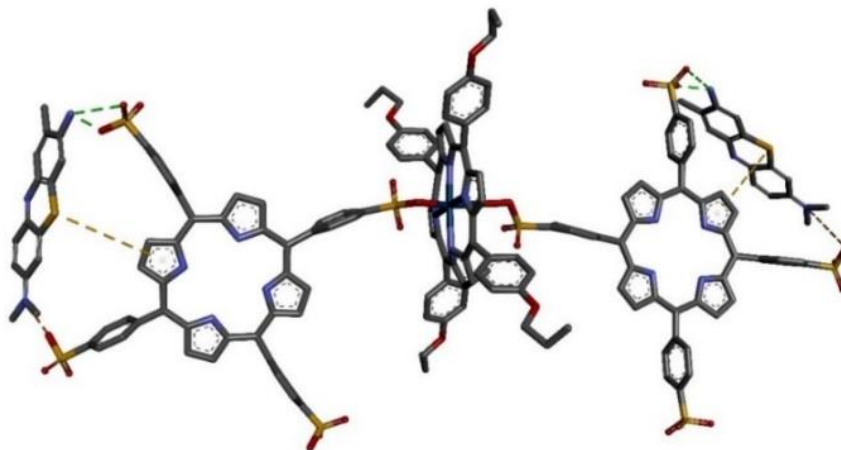


**Figure 13.** Proposed mechanism for TB detection using hetero-trimer as sensitive material. Atom color coding follows standard CPK rules: carbon-black, oxygen-red, nitrogen-blue, sulfur-yellow, platinum-dark blue, hydrogen-white.

**The fluorescent sensor for the detection of toluidine blue is the first designed to test concentrations of the dye intensively used in medical imaging, because a concentration level greater than 50  $\mu\text{M}$  of TB produces carcinogenic effects in any cell type.**

The research results were published in ISI Chemosensors journal: Lascu A, **Epuran C**, Fratilescu I, Birdeanu M, Halip L, Fagadar-Cosma E. Porphyrin Hetero-Trimer Involving a Hydrophilic and a Hydrophobic Structure with Application in the Fluorecent Detection of Toluidine Blue. *Chemosensors*, **2022**; 10 (11) 481. <https://doi.org/10.3390/chemosensors10110481> (FI= 4229).

Another notable result is the realization of a new type of citrate-selective potentiometric sensor, using Pt(II)-carboxy-phenyl-tris-(phenoxy-phenyl)-porphyrin as ionophore in the formulation of polyvinyl chloride (PVC) membranes differently plasticized with: o-nitrophenyloctyl ether (NPOE), dioctyl phthalate (DOP) and dioctyl sebacate (DOS). The performance of each sensor was tested by measuring its potential in the concentration decade from  $10^{-6}$ – $10^{-1}$  M in ten different solutions of anions:  $\text{F}^-$ ,  $\text{Br}^-$ ,  $\text{I}^-$ ,  $\text{ClO}_4^-$ ,  $\text{SCN}^-$ ,  $\text{NO}_2^-$ ,  $\text{NO}_3^-$ , Citrate $^{3-}$ ,  $\text{Sal}^-$ , Acetate $^-$ . ***The PVC membrane plasticized with dioctylsebacate (DOS), was the best one for desingning the citrate-selective sensor, that precisely functioned in the concentration domain of  $5 \times 10^{-7}$ – $1 \times 10^{-1}$  M citrate.*** The Nernstian slope (19.73 mV/decade), the very- good selectivity of the membrane towards a set of interfering anions and a five weeks lifetime recommend this

sensor for quantitative determination of citrate from synthetic samples and food supplements (magnesium citrate, calcium citrate and magnesium citrate in tablet form).

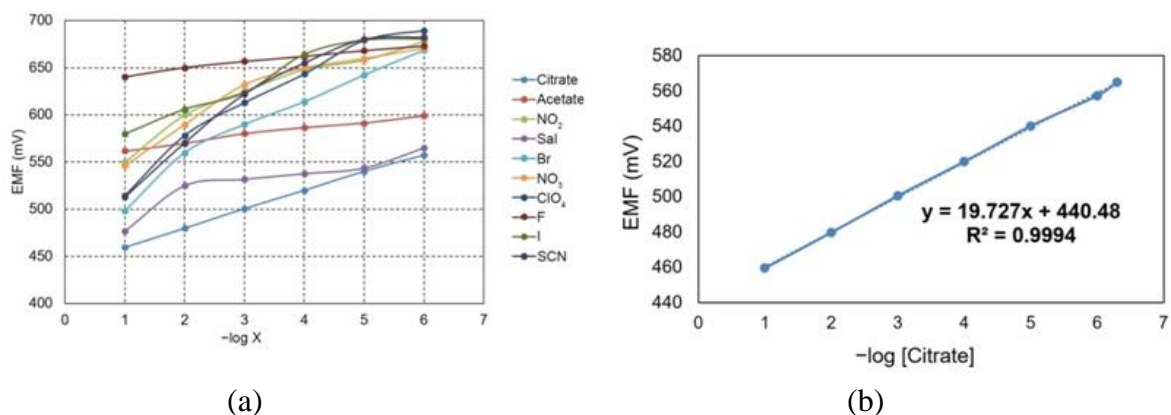


**Figure 14.** The potentiometric response of sensor to different anions (a); potentiometric response of sensor to citrate ion (b).

The mechanism of recognition is based on the interactions between the porphyrin and the citrate anions, which implies mainly the platinum atom located in the core of the porphyrin molecule. The three possible ways to bind citrate are:  $\pi$ -anion interactions (orange in Figure 15),  $\pi - \pi$  interactions (green in Figure 15) and Colombian interactions (yellow in Figure 15),

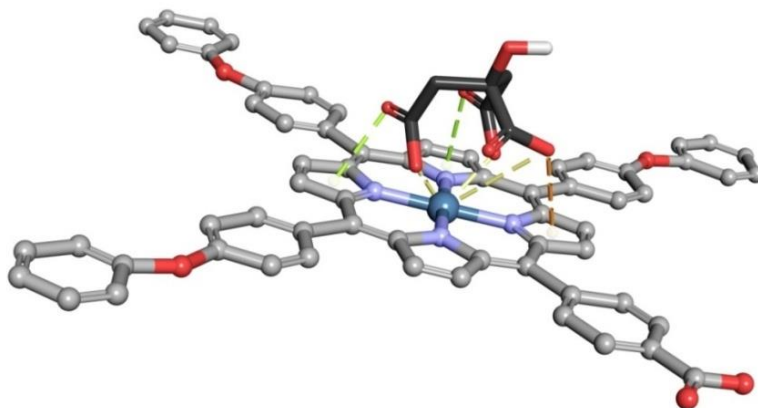


**Figure 15.** Representation of possible interactions between citrate ion and Pt(II)-COOH-TPOPP, used as an ionophore.

The results of the study were published in the journal *ISI Chemosensors*: Vlascici, D.; Lascu, A.; Fratilesco, I.; Anghel, D.; **Epuran, C.**; Birdeanu, M.; Chiriac, V.; Fagadar-Cosma, E. Asymmetric Pt(II)-Porphyrin Incorporated in a PVC Ion-Selective Membrane for the

In **Chapter 6**, the current performances of using different materials to detect/capture carbon dioxide are presented. For this purpose, the following materials (5-COOH-3MPP)-k-carrageenan and 5-COOH-3MPP-k-carrageenan functionalized with AuNPs (5-COOH-3MPP)-k-carrageenan-AuNPs) have been used and the functionality of the composite material complexed with AuNPs was extended for the detection of toxic  $Mn^{2+}$  ions.

A very small quantity of the composite material (5-COOH-3MPP)-k-carrageenan (1 g) can capture 6.97 mmol  $CO_2$ . This result is among the best performances reported till now in the literature, presenting the amazing advantage of working under normal conditions.

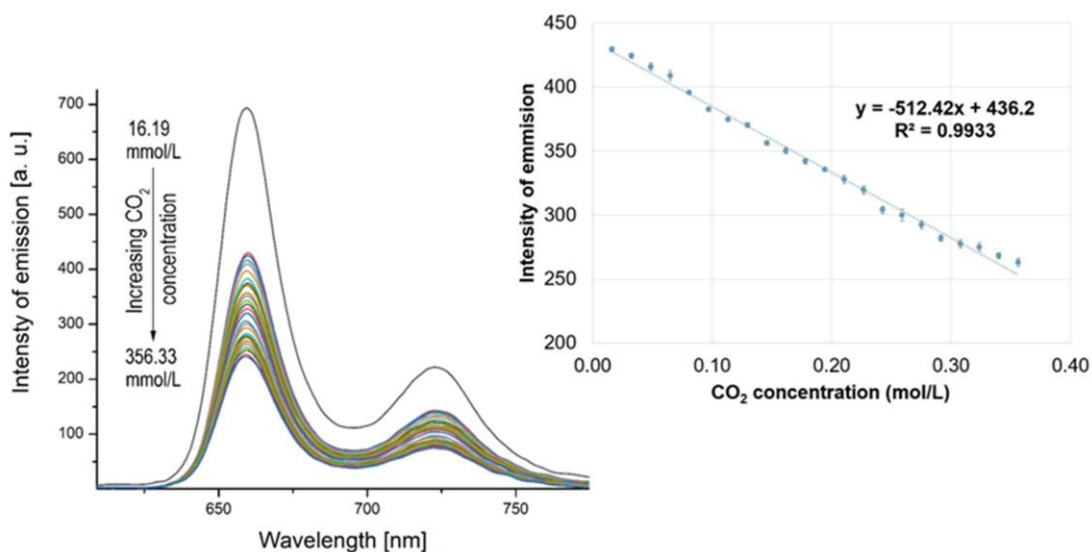


**Figure 16.** Overlapped emission spectra of the composite material after exposure to  $CO_2$ . The linear dependence between the emission intensity of the (5-COOH-3MPP)-k-carrageenan composite material (measured at 660 nm) and the  $CO_2$  concentration (10 mL/min flow), in a humid environment.

AFM investigation of the composite material (5-COOH-3MPP)-k-carrageenan deposited from DMF-water mixture on silica plates, have been performed (Figure 17 a) before treatment with  $CO_2$  and reveals a random porous surface with mountain type aggregates (height distribution 6.70-13.2 nm). After treatment with  $CO_2$ , the AFM images of 5-COOH-3MPP-k-carrageenan composite material (Figure 17 b) show larger aggregates, confirming the hypothesis. That  $CO_2$  was incorporated into the gel voids. The most important aspect is the self-organization into parallel rows of columns.



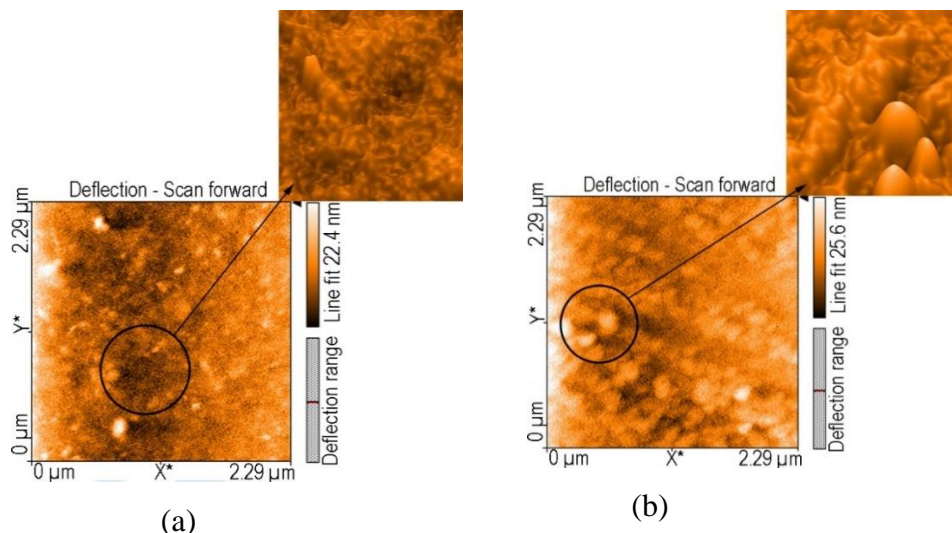


**Figure 17.** The 2D and 3D AFM images of (5-COOH-3MPP)-k-carrageenan composite material (a) and (5-COOH-3MPP)-k-carrageenan composite material after capturing CO<sub>2</sub> gas, in liquid DMF-water mixture (b).

In the permanent search to discover multifunctional materials, the detection of Mn<sup>2+</sup> ions is another application of the same material, after functionalization with AuNPs. The quantification of excess manganese in polluted water sources or in humans is important in prevention of toxicity diseases, such as manganism. By UV-Vis spectrometry, the porphyrin-k-carrageenan-AuNPs complex nanomaterial precisely detected Mn<sup>2+</sup> ions in solution in the concentration domain from 4.56×10<sup>-5</sup> M to 9.39×10<sup>-5</sup> M (5–11 mg/L).

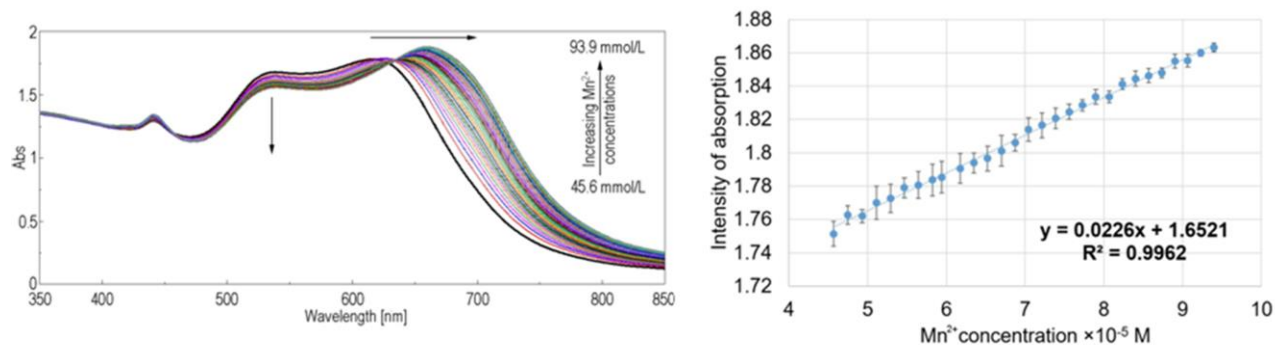


**Figure 18.** Overlapped UV-Vis spectra of Mn<sup>2+</sup> detection using (5-COOH-3MPP)-k-carrageenan-AuNPs hybrid material, in DMF/water and the Linear dependence between the intensity of absorption of (5-COOH-3MPP)-k-carrageenan-AuNPs hybrid material measured at 659 nm and the Mn<sup>2+</sup> ion concentration.

*The presented study was selected Cover Article by the journal ISI Chemosensors:*  
**Epuran C.;** Fratilescu I.; Măcsim A.-M.; Lascu A.; Ianasi C.; Birdeanu M.; Fagadar-Cosma E.



Excellent Cooperation between Carboxyl-Substituted Porphyrins,  $\kappa$ -Carrageenan and AuNPs for Extended Application in CO<sub>2</sub> Capture and Manganese Ion Detection. *Chemosensors*, **2022**, 10(4), 133. <https://doi.org/10.3390/chemosensors10040133>. (FI= 4229).

In **Chapter 7** the main purpose was to realize a new sensor for optically detection of uric acid from biological samples, by using as sensitive materials: hybrid nanomaterials consisting in 5,10,15,20-tetrakis(4-amino-phenyl)-porphyrin (TAmPP) alone or complexed with copper nanoparticles (CuNPs), platinum nanoparticles (PtNPs), or mixed type (Pt@CuNPs) for improving the detection range.

The hybrid material generated by complexation of porphyrin with PtNPs (*TAmPP-PtNPs*) gave the best performance for uric acid detection domain  $6.1958 \times 10^{-6} - 1.5763 \times 10^{-5}$  M. The sensor proved its selectivity even in the presence of 100-times more concentrations of the interference species (glucose (Glu), ascorbic acid (AA), NaCl, KCl, CH<sub>3</sub>COONa, MgSO<sub>4</sub>, KI, lactic acid (LA), sodium salicylate (SS)) that are usually present in human body.

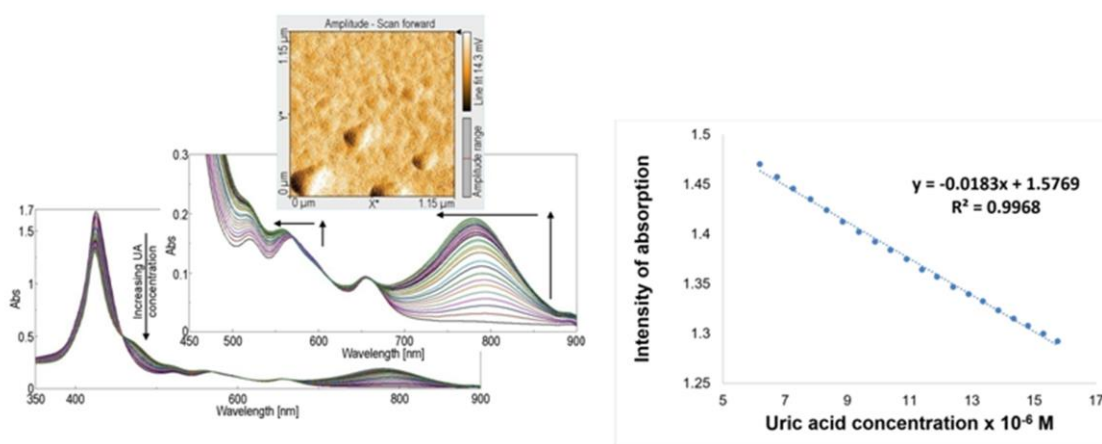


**Figure 19.** Superimposed UV-Vis spectra of the TAmPP-PtNPs complex during the addition of uric acid (a); linear dependence between the absorption intensity of the TAmPP-PtNPs hybrid material and the concentration of uric acid (b).

All materials described in this work can be successfully used for the detection of uric acid for human monitoring in a complementary range between  $0.582 \times 10^{-6} - 1.5763 \times 10^{-5}$  M UA concentrations (Figure 20). The trace detection was realized by TAmPP alone (a LOF of 0.28 μM UA).

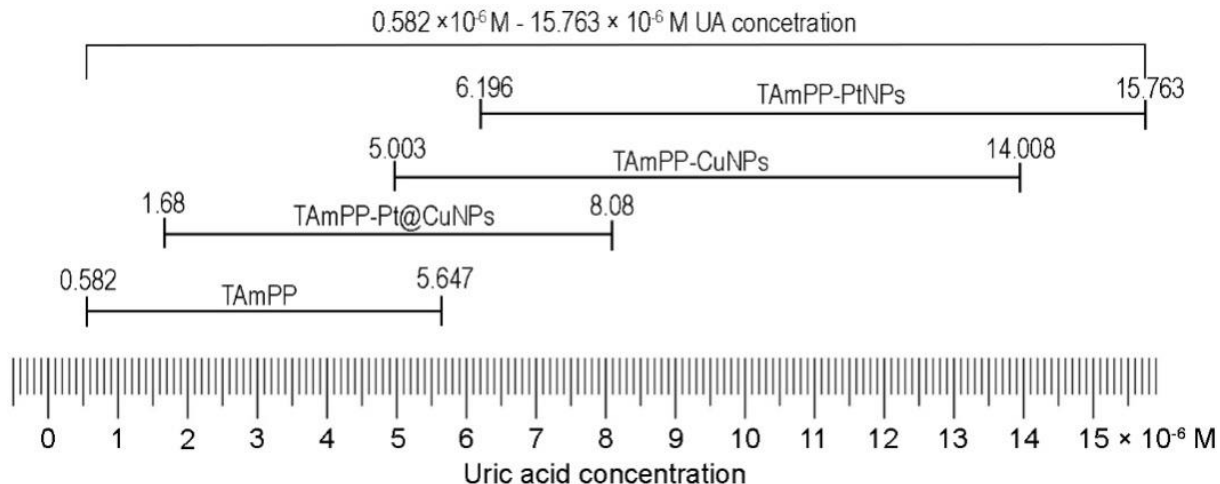


**Figure 20.** The range of uric acid detection covered by the TAmPP-containing materials used in this study.

*The results were published and selected as a Feature Paper in the journal ISI Processes: Epuran, C.; Fratilescu, I.; Anghel, D.; Birdeanu, M.; Orha, C.; Fagadar-Cosma, E. A Comparison of Uric Acid Optical Detection Using as Sensitive Materials an Amino-Substituted Porphyrin and Its Nanomaterials with CuNPs, PtNPs and Pt@CuNPs. Processes, 2021, 9 (11), 2072. <https://doi.org/10.3390/pr9112072>.*

**Chapter 8** presents the development of new corrosion inhibitors based on sandwich-type layered films on the surface of steel electrodes. The layers contained MnTa<sub>2</sub>O<sub>6</sub>, and two different substituted porphyrin derivatives, namely: 5-(4-carboxy-phenyl)-10,15,20-tris(4-methyl-phenyl)-porphyrin and its ester 5-(4-methyl-benzoate)-10,15,20-tris(4-methyl-phenyl)-porphyrin, which are novel compounds. The electrochemical measurements for all different order of depositing materials (Figure 21) evidenced in all cases an efficiency of corrosion inhibition from 65.6 to 83.7%, that depends on the type of the porphyrin and its first or second position on the steel.

The best performance (83.7%) was realized by the MAPLE/PLD laser deposition of 5-(4-carboxy-phenyl)-10,15,20-tris(4-methyl-phenyl)-porphyrin/MnTa<sub>2</sub>O<sub>6</sub> (h), justified by the physical mechanism of adsorbing and blocking the acid towards the surface of steel electrodes.

Electrod	E (I=0) (mV)	R <sub>p</sub> (Ωcm <sup>2</sup> )	i <sub>corr</sub> (mA/cm <sup>2</sup> )	β <sub>a</sub> (mV)	β <sub>c</sub> (mV)	v <sub>corr</sub> (mm/Y)	IE (%)
OL	-414.1	88.53	1.2924	258.0	-263.5	1.511	-
a	-430.0	130.72	0.4440	84.1	-85.9	0.5192	65.64
b	-449.9	139.39	0.3401	79.2	-81.1	0.3977	73.68
c	-440.0	131.76	0.4118	82.7	-84.1	0.5067	68.13
d	-502.8	159.67	0.2101	71.5	-72.4	0.2458	83.74
e	-477.1	150.44	0.2573	75.8	-77.2	0.3010	80.09
f	-488.4	154.53	0.2380	73.2	-74.8	0.2784	81.58
g	-469.8	146.42	0.2677	77.3	-79.3	0.3131	79.28

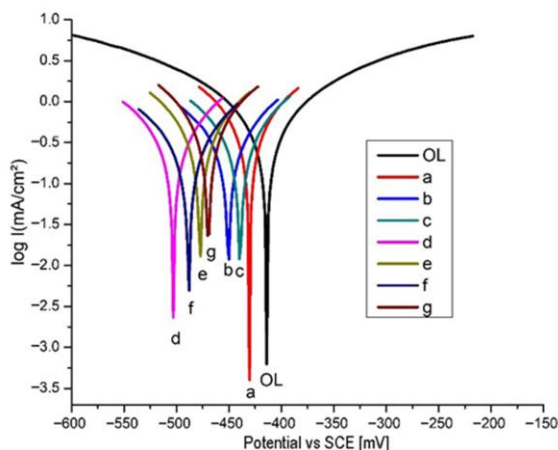


**Figure 21.** Tafel parameters for the investigated steel electrodes (protected and unprotected) and Tafel polarization curves recorded in 0.1 M HCl medium for the studied thin films: OL bars W1.4043; a) MnTa<sub>2</sub>O<sub>6</sub>(h); b) 5-(4-carboxy-phenyl)-10,15,20-tris(4-methyl-phenyl)-porphyrin; c) 5-(4-methyl-benzoate)-10,15,20-tris (4-methyl-phenyl)-porphyrin; d) 5-(4-carboxy-phenyl)-10,15,20-tris (4-methyl-phenyl)-porphyrin / MnTa<sub>2</sub>O<sub>6</sub>(h); e) MnTa<sub>2</sub>O<sub>6</sub> (h) / 5-(4-carboxy-phenyl)-10,15,20-tris (4-methyl-phenyl)-porphyrin; f) 5-(4-methyl-benzoate)-10,15,20-tris (4-methyl-phenyl)-porphyrin/ MnTa<sub>2</sub>O<sub>6</sub> (h); g) MnTa<sub>2</sub>O<sub>6</sub>(h) / 5-(4-methyl-benzoate)-10,15,20-tris (4-methyl-phenyl)-porphyrin.

The superior result of the porphyrin functionalized with COOH is illustrated in the SEM image (Figure 22) representing the perpendicular section of the steel electrode covered with 5-(4-carboxy-phenyl)-10,15,20-tris(4-methyl-phenyl)-porphyrin/MnTa<sub>2</sub>O<sub>6</sub> (h). It is obvious that the coverage is adherent and has uniform thickness (between 20 and 30 microns).

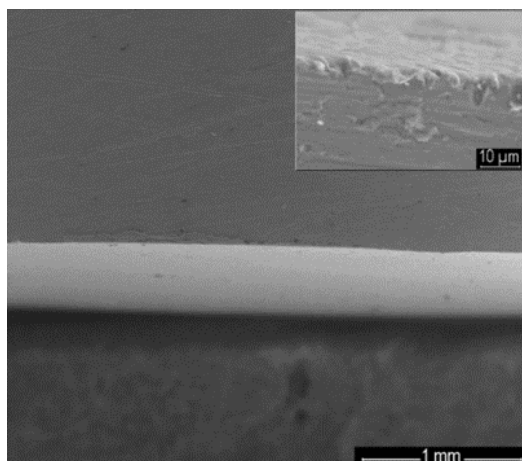


**Figure 22.** SEM image of the vertical section of the steel electrode coated with 5-(4-carboxy-phenyl)-10,15,20-tris(4-methyl-phenyl)-porphyrin/MnTa<sub>2</sub>O<sub>6</sub>(h).

In the case of double substitution with COOH groups, an important effect that has been studied is brought about by the position of the two COOH groups (*cis* or *trans*) on the porphyrinic cycle. The best performance in corrosion inhibition of 91.76% was exhibited by the steel protected with a double layer, firstly covered with 5,15-(4-carboxy-phenyl)-10,20-bisphenyl-porphyrin and secondly with MnTa<sub>2</sub>O<sub>6</sub>. The porphyrin with a smaller steric hindrance 5,15-(4-carboxy-phenyl)-10,20-bisphenyl-porphyrin, can generate much more uniform supramolecular aggregates due to the presence in *trans* of two COOH groups. The *trans* -COOH porphyrin is acting better than the porphyrin with the COOH groups in *cis* vicinal position, that has large voids in its covered surface.

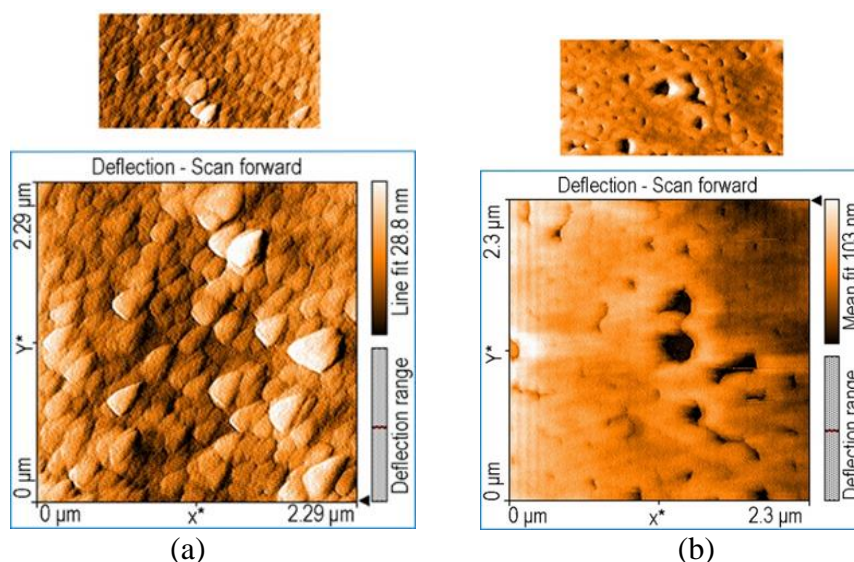


**Figure 23.** AFM images showing better coverage realized by *trans* 5,15-(4-carboxy-phenyl)10,20-bisphenyl-porphyrin (a) in comparison with *cis* structure, 5,10-(4-carboxy-phenyl)-15,20-(4phenoxy-phenyl)-porphyrin (b).

*This study was part of the activities of the Project PN-III-P2-2.1-PED-2019-0487, 528 PED/2020 CERAPOR-CORR, "Ceramic / porphyrin hybrid materials deposited as single or sandwich layers by the PLD technique for corrosion inhibition of steels in acid environment", in whose team I was a member, having a specific role throughout the duration of the project.*

The results of the project were published in the ISI indexed works:

- Birdeanu, M.; *Epuran, C.*; Fratilescu, I.; Fagadar-Cosma, E. Structured Thin Films Based on Synergistic Effects of MnTa<sub>2</sub>O<sub>6</sub> Oxide and bis-Carboxy-phenyl-substituted Porphyrins, Capable to Inhibit Steel Corrosion. *Processes* **2021**, *9*, 1890. <https://doi.org/10.3390/pr911189>.

- Birdeanu, M.; Fratilescu, I.; *Epuran, C.*; Murariu, A.C.; Socol, G.; Fagadar-Cosma, E. Efficient Decrease in Corrosion of Steel in 0.1 M HCl Medium Realized by a Coating with Thin Layers of MnTa<sub>2</sub>O<sub>6</sub> and Porphyrins Using Suitable Laser-Type Approaches. *Nanomaterials* **2022**, 12, 1118. <https://doi.org/10.3390/nano12071118>.

## General conclusions

This thesis brings as novel elements the obtaining and fully characterization of new porphyrinic structures: porphyrins-bases, metalloporphyrins and a hetero-trimer type compound. Their various applications towards the realization of new more efficient fluorometric, potentiometric and optical sensors and identification of inhibitors suited for corrosion protection were the second main objective of this thesis.

The novel porphyrin structures of type A<sub>3</sub>B and A<sub>2</sub>B<sub>2</sub> that were obtained by the multicomponent Adler-Longo method and fully characterized, are:

- *5-(methyl-4-benzoate)-10,15,20-tris-(4-methyl-phenyl)-porphyrin;*
- *5-(4-carboxy-phenyl)-10,15,20-tris-(4-methyl-phenyl)-porphyrin;*
- *5-(4-carboxy-phenyl)-10,15,20-tris-(4-phenoxy-phenyl)-porphyrin;*
- *5,10-(4-carboxy-phenyl)-15,20-(4-phenoxy-phenyl)-porphyrin (cis).*

The obtained structure were characterized by TLC, MS, UV-Vis, <sup>1</sup>H-NMR <sup>13</sup>C-NMR and FT-IR.

*The new structure of a hetero-trimer, Pt-allyloxyPP-TSPP*, was obtained by binding two molecules of 5,10,15,20-tetra-(4-sulfonato-phenyl)-porphyrin (TSPP) to one molecule of Pt(II)-5,10,15,20-tetra-(4-allyloxy-phenyl)-porphyrin (Pt-allyloxy-PP), and proved its capacity to fluorimetrically detect toluidine blue in trace.

*The new porphyrinic hetero-trimer (Pt-allyloxyPP-TSPP)* detected toluidine blue in the linear concentration range  $1.9 \times 10^{-6} - 6.39 \times 10^{-5}$  M with a relevant detection limit of 1.4  $\mu$ M for biological investigations. *This study highlights the development of the first fluorescent sensor for toluidine blue (TB), designed specifically for testing trace concentrations in medical samples, as concentrations greater than 50  $\mu$ M of TB are known to produce carcinogenic effects in any cell type. This achievement will allow monitoring remaining toxic dyes after imagistic tests.*

Another successful approach was the use of *Pt(II)-5-(4-carboxy-phenyl)-10,15,20-tris-(4-phenoxy-phenyl)-porphyrin* as ionophore in PVC plasticized with dioctyl sebacate (DOS), with the purpose to obtain a potentiometric sensor capable of detecting *citrate anion* (important for pharmaceutical and food monitoring). The potentiometric response was linear in the range of  $5 \times 10^{-7} - 1 \times 10^{-1}$  M citrate, with a Nernstian response and a detection limit of  $3 \times 10^{-7}$  M with great stability in time (five weeks).

A third objective of this work was to obtain hybrid or composite materials that due to their synergistic behaviour might potentiate different optical or chemical properties of the incorporated porphyrins.

Thus, the composite material (*5-COOH-3MPP*)-*k-carrageenan* has been shown to be sensitive to CO<sub>2</sub> (recognition and quantification by both UV-Vis and fluorescence spectroscopy) and *is able to capture 6.97 mmol CO<sub>2</sub> / 1 g of material adsorbent, being rated among the best adsorbent materials reported in the specialized literature, with the mention that it worked simply and safely, under normal conditions.*

*The same composite material, this time functionalized with gold nanoparticles (porphyrin-k-carrageenan-AuNPs)* detected by spectroscopic methods Mn<sup>2+</sup> ions in solution, with high precision (99.62%) in the concentration range from  $4.56 \times 10^{-5}$  M to  $9.39 \times 10^{-5}$  M ( $5 \div 11$  mg/L). This sensor can be used for manganism disease monitoring.

*Another class of new inorganic-organic hybrid nanomaterials were obtained* by complexing a symmetrical amino-substituted porphyrin (5,10,15,20-tetrakis-(4-amino-phenyl)-porphyrin, (TAmPP)) with mixed colloidal metal nanoparticles: PtNPs, CuNPs or Pt@CuNPs with the aim of achieving materials capable to bind and recognize uric acid. All synthesized hybrid materials have been applied to complementary detect uric acid (UA) in human fluids in a concentration range between  $0.582 \times 10^{-6} - 1.5763 \times 10^{-5}$  M UA. The complexation of porphyrin with metal nanoparticles such as CuNPs, PtNPs or mixed nanoparticles with Cu core and Pt shell (Pt@CuNPs) increased the detection range, shifting it to higher concentrations.

Another direction of research presented in this thesis is the *development of materials based on porphyrins and pseudo-binary oxide MnTa<sub>2</sub>O<sub>6</sub>, that can be deposited as double layered thin films on carbon-steel and have corrosion inhibition properties.*

The capacity of 5-(4-carboxy-phenyl)-10,15,20-tris-(4-methyl-phenyl)-porphyrin, grafted with a -COOH functional group (providing better hydrophilicity and enabling the creation of



extended hydrogen bonds) performed better corrosion inhibition capacity (IE= 83.7%) than its ester, 5-(4-methyl-benzoate)-10,15,20-tris(4-methyl-phenyl)-porphyrin (IE= 68.13%), when both were deposited by the same method, in the same order on the steel surface.

**The best corrosion inhibition efficiency of 91.76%** was realized by the steel coated with a mixed layer consisting of 5,15-(4-carboxy-phenyl)-10,20-phenyl-porphyrin/ MnTa<sub>2</sub>O<sub>6</sub> (s), deposited by the drop-casting method, due to the trans conformation of the porphyrin, that confers better self-assembling properties. The lowest value of the inhibition efficiency (IE= 60.40%) was recorded for the monolayer of pseudo-binary oxide MnTa<sub>2</sub>O<sub>6</sub> deposited by the drop-casting method, proving the importance of the porphyrinic component in the composition of the films.

## References

1. Villari, V.; Gaeta, M.; D'Urso, A.; Micali, N. Porphyrin/carbon nanodot supramolecular complexes and their optical properties. *Colloids Surf. A: Physicochem. Eng.* **2022**, *648*, 129436. <https://doi.org/10.1016/j.colsurfa.2022.129436>
2. Fringu, I.; Lascu, A.; Măcsim, A.M.; Fratilescu, I.; Epuran, C.; Birdeanu, M.; Fagadar-Cosma E. Pt(II)-A<sub>2</sub>B<sub>2</sub> metalloporphyrin-AuNPS hybrid material suitable for optical detection of 1-anthraquinon sulfonic acid. *Chem. Pap.* **2022**, *76*, 2513–2527. <https://doi.org/10.1007/s11696-021-02047-2>
3. Lascu, A.; Epuran, C.; Fratilescu, I.; Birdeanu, M.; Halip, L.; Fagadar-Cosma E. Porphyrin Hetero-Trimer Involving a Hydrophilic and a Hydrophobic Structure with Application in the Fluorescent Detection of Toluidine Blue. *Chemosensors* **2022**, *10*, 481. <https://doi.org/10.3390/chemosensors10110481>
4. Somkuwar, P.; Bhaskar, R.; Ramasamy, S.K.; Shaji, L.K.; Bhat, S.G.; Jose, J.; Kumar, A.; Kalleshappa, A.S. Porphyrin-based NIR Fluorescent Probe for Bi<sup>3+</sup> and Potential Applications. *J Fluoresc.* **2023**. <https://doi.org/10.1007/s10895-023-03315-y>
5. Özbek, O. A potentiometric sensor for the determination of potassium in different baby follow-on milk, water, juice and pharmaceutical samples. *J. Food Compos. Anal.* **2023**, *115*, 104937. <https://doi.org/10.1016/j.jfca.2022.104937>
6. Munawaroh, H.S.H.; Sunarya, Y.; Anwar, B.; Priatna, E.; Risa, H.; Koyande, A.K.; Show, P.-L. Protoporphyrin Extracted from Biomass Waste as Sustainable Corrosion Inhibitors of T22 Carbon Steel in Acidic Environments. *Sustainability* **2022**, *14*, 3622. <https://doi.org/10.3390/su14063622>

7. Silvestri, S.; Fajardo, A.R.; Iglesias, B.A. Supported porphyrins for the photocatalytic degradation of organic contaminants in water: a review. *Environ Chem Lett.* **2022**, *20*, 731–771. <https://doi.org/10.1007/s10311-021-01344-2>
8. Liu, Q.; Sun, Q.; Shen, J.; Li, H.; Zhang, Y.; Chen, W.; Yu, S.; Li, X.; Chen Y. Emerging tetrapyrrole porous organic polymers for chemosensing applications. *Coord. Chem. Rev.* **2023**, *482*, 215078. <https://doi.org/10.1016/j.ccr.2023.215078>
9. Gottfried, J.M. Surface chemistry of porphyrins and phthalocyanines. *Surf. Sci. Rep.* **2015**, *70*, 259–379. <https://doi.org/10.1016/j.surfrep.2015.04.001>
10. Balaban, T.S.; Goddard, R.; Linke-Schaetzel, M.; Lehn, J.-M. 2-Aminopyrimidine Directed Self-Assembly of Zinc Porphyrins Containing Bulky 3,5-Di-tert-butylphenyl Groups. *J.Am.Chem.Soc.* **2003**, *125*, 4233–4239. <https://doi.org/10.1021/ja029548r>
11. Vlascici, D.; Fagadar-Cosma, E.; Popa, I.; Chiriac, V.; Gil-Augusti, M. A Novel Sensor for Monitoring of Iron(III) Ions Based on Porphyrins. *Sensors* **2012**, *12*, 8193–8203. <https://doi.org/10.3390/s120608193>
12. Öztürk, N.; Çırak, Ç.; Bahçeli, S. FT-IR Spectroscopic Study of 1,5-Pentanedithiol and 1,6-Hexanedithiol Adsorbed on NaA, CaA and NaY Zeolites. *Z. Naturforsch. A.* **2014**, *60*, 633–636. <https://doi.org/10.1515/zna-2005-8-913>
13. Wen, P.; Gong, P.; Mi, Y.; Wang, J.; Yang, S. Scalable fabrication of high quality graphene by exfoliation of edge sulfonated graphite for supercapacitor application. *RSC Adv.* **2014**, *4*, 35914–35918. <https://doi.org/10.1039/C4RA04788E>
14. Boukir, A.; Fellak, S.; Doumenq, P. Structural characterization of *Argania spinosa* Moroccan wooden artifacts during natural degradation progress using infrared spectroscopy (ATR-FTIR) and X-Ray diffraction (XRD). *Heliyon* **2019**, *5*, e02477. <https://doi.org/10.1016/j.heliyon.2019.e0247747>
15. Wang, M.Y.; Zhu, W.; Wang, Q.; Yang, Y.; Zhou, H.; Zhang, F.; Zhou, L.; Razal, J.M.; Wallace, G.G.; Chen, J. Metal porphyrin intercalated reduced graphene oxide nanocomposite utilized for electrocatalytic oxygen reduction. *Green Energy Environ.* **2017**, *2*, 285–293. <https://doi.org/10.1016/j.gee.2017.06.001>
16. Chen, B.-K., Su, C.-T., Tseng, M.-C.; Tsay, S.-Y. Preparation of Polyetherimide Nanocomposites with Improved Thermal, Mechanical and Dielectric Properties. *Polymer Bulletin* **2006**, *57*, 671–681. <https://doi.org/10.1007/s00289-006-0630-3>



17. Mak, C.A.; Pericas, M.A.; Fagadar-Cosma, E. Functionalization of A3B-type porphyrin with Fe<sub>3</sub>O<sub>4</sub> MNPs. Supramolecular assemblies, gas sensor and catalytic applications. *Catal. Today* **2018**, *306*, 268–275. <https://doi.org/10.1016/j.cattod.2017.01.014>
18. Nomoto, A.; Mitsuoka, H.; Ozeki, H.; Kobuke, Y. Porphyrin hetero-dimer as charge separating system for photocurrent generation. *Chem. Commun.* **2003**, *9*, 1074–1075. <https://doi.org/10.1039/b300456b>
19. Habets, T.; Lensen, D.; Speller, S.; Elemans, J.A. Self-assembly of covalently linked porphyrin dimers at the solid–liquid interface. *Molecules* **2019**, *24*, 3018. <https://doi.org/10.3390/molecules24163018>.

## PAPERS PUBLISHED IN THE FIELD OF THE DOCTORAL THESIS

The process of disseminating the results obtained in the framework of the research carried out in the field of the doctoral thesis was highlighted by the realization of the following series of significant actions:

### A. List of published works from the doctoral thesis material

*I. Publications in international journals indexed by ISI and indexed in the Web of Science database:*

**\*\*\* total number of citations according to Web of Science= 25**

**\*\*\* 7 scientific articles, of which two are first author, with a cumulative impact factor equal to 25.251**

1. Dana Vlascici, Anca Lascu, Ion Fratilescu, Diana Anghel, **Camelia Epuran**, Mihaela Birdeanu, Vlad Chiriac, Eugenia Fagadar-Cosma. Asymmetric Pt(II)-Porphyrin Incorporated in a PVC Ion-Selective Membrane for the Potentiometric Detection of Citrate. *Chemosensors* **2023**, *11*, 108. <https://doi.org/10.3390/chemosensors11020108>. **FI= 4.229.**
2. Anca Lascu, **Camelia Epuran**, Ion Fratilescu, Mihaela Birdeanu, Liliana Halip, Eugenia Fagadar-Cosma. Porphyrin hetero-trimer involving a hydrophilic and a hydrophobic structure with application in the fluorescent detection of toluidine blue. *Chemosensors* **2022**, *10*, 48. <https://doi.org/10.3390/chemosensors10110481>. **FI= 4.229.**

3. Mihaela Birdeanu, **Camelia Epuran**, Ion Fratilescu, Eugenia Fagadar-Cosma. Structured composites between  $MnTa_2O_6$  and porphyrins: Influence of the number of carboxylic groups grafted on porphyrins on the capacity to inhibit corrosion of steel.  
*Indian J. Chem. Technol.* **2022**, 29, 354–366.  
<https://doi.org/10.56042/ijct.v29i4.59344>. **FI= 0.56.**
4. **Epuran Camelia**, Fratilescu Ion, Macsim Ana Maria, Lascu Anca, Ianasi Catalin, Birdeanu Mihaela, Fagadar-Cosma Eugenia. Excellent Cooperation between Carboxyl-Substituted Porphyrins, k-Carrageenan and AuNPs for Extended Application in  $CO_2$  Capture and Manganese Ion Detection. *Chemosensors* **2022**, 10, 133.  
<https://doi.org/10.3390/chemosensors10040133>. Premiat ca și **Cover Article**. **FI= 4.229.**
5. Birdeanu Mihaela, Fratilescu Ion, **Epuran Camelia**, Murariu Alin Constantin, Socol Gabriel, Fagadar-Cosma Eugenia. Efficient Decrease in Corrosion of Steel in 0.1 M HCl Medium Realized by a Coating with Thin Layers of  $MnTa_2O_6$  and Porphyrins Using Suitable Laser-Type Approaches. *Nanomaterials* **2022**, 12, 1118.  
<https://doi.org/10.3390/nano12071118> **FI= 5.3.**
6. **Camelia Epuran**, Ion Fratilescu, Diana Anghel, Mihaela Birdeanu, Corina Orha, Eugenia Fagadar-Cosma. A Comparison of Uric Acid Optical Detection Using as Sensitive Materials an Amino-Substituted Porphyrin and Its Nanomaterials with CuNPs, PtNPs and Pt@CuNPs. *Processes* **2021**, 9, 2072. <https://doi.org/10.3390/pr9112072>. Selectat ca **Feature Paper**. **FI= 3.352.**
7. Mihaela Birdeanu, **Camelia Epuran**, Ion Fratilescu, Eugenia Fagadar-Cosma. Structured Thin Films Based on Synergistic Effects of  $MnTa_2O_6$  Oxide and bis-Carboxy-phenyl-substituted Porphyrins, Capable to Inhibit Steel Corrosion. *Processes* **2021**, 9, 1890.  
<https://doi.org/10.3390/pr9111890>. **FI= 3.352.**

## *II. National patents approved and published*

1. **RO Patent–a202200130**, Birdeanu, M.; **Epuran, C.**; Frățilescu, I.; Fagadar-Cosma, E. Titlu: „Procedeu de obținere de inhibitori de coroziune organizați in straturi subțiri

alternative de porfirine substituie cu grupări carboxil și oxid pseudo-binar de tip  $\text{MnTa}_2\text{O}_6$ , realizate prin tehnica PLD”, published in **RO-BOPI 9/2023, din 29.09.2023**.

### ***III. Participation in international scientific events, in Romania with oral presentation***

**1. Camelia Epuran.** Improved domain and selectivity for uric acid detection using assensitive materials complexes between an amino functionalized porphyrin and CuNPs, PtNPs or Pt@CuNPs. ***ICMPP – OPEN DOOR TO THE FUTURE SCIENTIFIC COMMUNICATIONS OF YOUNG RESEARCHERS MacroYouth***’2021 2nd Edition, Iasi, November 19, 2021, pp 11.

**2. Camelia Epuran,** Ion Fratilescu, Diana Anghel, Mihaela Birdeanu, Eugenia Fagadar-Cosma. Selection of the best sensitive material for uric acid detection from complexes of afunctionalized porphyrin and CuNPs, PtNPs or Pt@CuNPs. ***New trends and strategies in the chemistry of advanced materials with relevance in biological systems, technique and environmental protection***” 13<sup>th</sup> Edition, online, October 07-08, 2021, pp 23.

### ***IV. Participation in international scientific events, abroad with oral presentation (co-author)***

**1. Mihaela Birdeanu, Camelia Epuran,** Ion Fratilescu, Eugenia Fagadar-Cosma. Thin film layers based on porphyrins and pseudo-binary-oxides with synergistic effects in corrosion inhibition of steel, ***International Conference on THIN-FILM Processing and Application*** (ICTFPA-2022), 04 - 05 March **2022**, MATS University, Arang, India.

### ***V. Participation in international scientific events, in Romania with oral presentation (co-author)***

**1. Mihaela Birdeanu, Aurel-Valentin Birdeanu, Camelia Epuran,** Eugenia Fagadar-Cosma. New sandwich type materials based on  $\text{MnTa}_2\text{O}_6$  and carboxyl-substituted  $\text{A}_4$  and  $\text{A}_3\text{B}$  porphyrins. The effect of the carboxyl groups on corrosion inhibition properties. ***EmergeMAT 4<sup>th</sup> International Conference on Emerging Technologies in Materials Engineering***, 4-5 November 2021, Bucharest, Romania.

***VI. Participation and dissemination actions towards the public (scholar, students, interested persons)***

The exposition and explanations provided at the poster with the title Project PN-III-P2-2.1-PED-2019-0487, 528 PED/2020CERAPOR-CORR, "Ceramic / porphyrin hybrid materials deposited as single or sandwich layers by the PLD technique for corrosion inhibition of steels in acidic environment" and the graphic abstract from the paper published in Nanomaterials with the title "One A<sub>3</sub>B Porphyrin Structure-Three Successful Applications" (<https://doi.org/10.3390/nano12111930>). Event: The 18<sup>th</sup> edition of the Night of European Researchers event, funded by the European Commission through Marie Skłodowska-Curie actions, **September 30, 2022**.

**B. List of works with the complementary theme published as first author/co-author**

***I. Publications in international journals indexed by ISI and indexed in the Web of Science database:***

**\*\*\* total number of citations according to Web of Science= 48**

**\*\*\* 8 scientific articles, with a cumulative impact factor equal to 35.716**

1. Anca Lascu, Dana Vlascici, Mihaela Birdeanu, **Camelia Epuran**, Ion Fratilescu, Eugenia Fagadar-Cosma. The Influence of the Nature of the Polymer Incorporating the Same A<sub>3</sub>B Multifunctional Porphyrin on the Optical or Electrical Capacity to Recognize Procaine. *Int. J. Mol. Sci.* **2023**, *24*, 17265. <https://doi.org/10.3390/ijms242417265>. **FI= 5.6.**
2. Mihaela Birdeanu, Ion Fratilescu, **Camelia Epuran**, Liviu Mocanu, Catalin Ianasi, Anca Lascu, Eugenia Fagadar-Cosma. Nanomaterials Based on Collaboration with Multiple Partners: Zn<sub>3</sub>Nb<sub>2</sub>O<sub>8</sub> Doped with Eu<sup>3+</sup> and/or Amino Substituted Porphyrin Incorporated in Silica Matrices for the Discoloration of Methyl Red. *Int. J. Mol. Sci.* **2023**, *24*, 8920. <https://doi.org/10.3390/ijms24108920>. **FI= 5.6.**
3. Ion Fratilescu, Anca Lascu, Bogdan Ovidiu Taranu, **Camelia Epuran**, Mihaela Birdeanu, Ana-Maria Macsim, Eugenia Tanasa, Eugeniu Vasile, Eugenia Fagadar-Cosma. One A<sub>3</sub>B

- Porphyrin Structure—Three Successful Applications. *Nanomaterials* **2022**, *12*, 1930. <https://doi.org/10.3390/nano12111930>. Premiata ca Editors' *choice-cover article*. **FI= 5.3**.
4. Ionela Fringu, Anca Lascu, Ana-Maria Macsim, Ion Fratilescu, **Camelia Epuran**, Mihaela Birdeanu, Eugenia Fagadar-Cosma. Pt (II)-A2B2 metalloporphyrin-AuNPS hybrid material suitable for optical detection of 1-anthraquinonsulfonic acid. *Chemical Papers* **2022**, *76*, 2513–2527. <https://doi.org/10.1007/s11696-021-02047-2>. **FI= 2.41**.
  5. Ion Fratilescu, Zoltán Dudás, Mihaela Birdeanu, **Camelia Epuran**, Diana Anghel, Ionela Fringu, Anca Lascu, Adél Len, Eugenia Fagadar-Cosma. Hybrid Silica Materials Applied for Fuchsine B Color Removal from Wastewaters. *Nanomaterials* **2021**, *11*, 863. <https://doi.org/10.3390/nano1104086>. **FI= 5.719**.
  6. Diana Anghel, Anca Lascu, **Camelia Epuran**, Ion Fratilescu, Catalin Ianasi, Mihaela Birdeanu, Eugenia Fagadar-Cosma, Hybrid Materials Based on Silica Matrices Impregnated with Pt-Porphyrin or PtNPs Destined for CO<sub>2</sub> Gas Detection or for Wastewaters Color Removal. *Int. J. Mol. Sci.* **2020**, *21*, 4262. <https://doi.org/10.3390/ijms21124262>. **FI= 5.62**.
  7. Eugenia Fagadar-Cosma, Nicoleta Plesu, Anca Lascu, Diana Anghel, Maria Cazacu, Catalin Ianasi, Gheorghe Fagadar-Cosma, Ion Fratilescu, **Camelia Epuran**. Novel Platinum-Porphyrin as Sensing Compound for Efficient Fluorescent and Electrochemical Detection of H<sub>2</sub>O<sub>2</sub>. *Chemosensors* **2020**, *8*, 29. <https://doi.org/10.3390/chemosensors8020029>. **FI= 5.02**.
  8. Diana Anghel, Mihaela Birdeanu, Anca Lascu, **Camelia Epuran**, Eugenia Fagadar-Cosma. Amino-substituted porphyrins at the border of hybrid materials generation and platinum nanoparticles detection. *Studia Universitatis Babeş-Bolyai, Chemia* **2020**, *65*, 107–120. <https://doi.org/10.24193/subbchem.2020.2.09>. **FI= 0.447**.

## ***II. Publications in international open access journals***

1. Diana Anghel, Anca Lascu, Ion Fratilescu, Camelia Epuran, Nicoleta Plesu, Eugenia Făgădar-Cosma. Review about Main Requirements for Porphyrin Derivatives as Components of Dye Sensitized Solar Cells. *J. Sol. Energy* **2019**, *6*, 78–86. <https://doi.org/10.31875/2410-2199.2019.06.9>.

### ***III. National patents approved and published***

**1. RO Patent–a202000533**, Fratilescu, I.; Anghel, D.; **Epuran, C.**; Ianasi, C.; Fagadar-Cosma E. Titlu: „Metoda de Adsorbție a Coloranților din Ape Contaminate Utilizând Materiale Hibrade pe Bază de Silice Mezoporoasă care Încorporează Nanoparticule de Platină sau Pt(II)-tetra-(aliloxi-fenil)-porfirina”, published in **RO-BOPI 2/2022, din 28.02.2022.**

### ***IV. Participation in international scientific events, abroad with poster***

- 1. Camelia Epuran**, Diana Anghel, Anca Lascu, Ion Fratilescu, Eugenia Fagadar-Cosma. Optical Detection of Rhodamine B by Pt(II) Tetra-(4-Allyloxy-Phenyl)-Porphyrin. *Proceedings of the 25<sup>th</sup> International Symposium on Analytical and Environmental Problems*, Szeged, Hungary, 2019, pp 129-132, ISBN 978-963-306-702-4.
- Ion Fratilescu, Diana Anghel, Anca Lascu, **Camelia Epuran**, Eugenia Fagadar-Cosma. Platinum-Porphyrin Involved in the UV-Vis Spectrophotometric detection of Rhodamine B and Oxygen Peroxide. *Proceedings of the 25<sup>th</sup> International Symposium on Analytical and Environmental Problems*, Szeged, Hungary, 2019, pp 133-136, ISBN 978-963-306-702-4.
- Diana Anghel, Anca Lascu, Ion Fratilescu, **Camelia Epuran**, Eugenia Fagadar-Cosma. Zn-Metalloporphyrins Containing Pyridyl Groups and Their Comparative Capacity to Coordinate Hexachloroplatinic Acid. *Proceedings of the 25<sup>th</sup> International Symposium on Analytical and Environmental Problems*, Szeged, Hungary, 2019, pp 100-103, ISBN 978-963-306-702-4.

### ***V. Participation in international scientific events, in Romania with a poster***

- 1. Camelia Epuran**, Ion Fratilescu, Diana Anghel, Anca Lascu, Eugenia Fagadar-Cosma. Complex between an A<sub>3</sub>B porphyrin, aurophilic and κ-carrageenan used for detection of 1-methylimidazole. *The 15<sup>th</sup> Edition of the Conference "New Trends in Chemistry Research"*, September, 21-22, **2023**, Timisoara, Romania pp.68.
- Ion Fratilescu, **Camelia Epuran**, Diana Anghel, Anca Lascu, Eugenia Fagadar-Cosma. Advanced antibacterial compounds. complexes between 1-methylimidazole and a carboxy–A<sub>3</sub>B porphyrin. *The 15<sup>th</sup> Edition of the Conference "New Trends in Chemistry Research"*, September, 21-22, **2023**, Timisoara, Romania, pp.69.

3. Diana Anghel, Anca Lascu, Ion Fratilescu, **Camelia Epuran**, Eugenia Fagadar-Cosma. New approaches to biological imaging coordination of boron compounds to different porphyrins for laser dyes and fluorescent labeling. *The 15<sup>th</sup> Edition of the Conference "New Trends in Chemistry Research"*, September, 21-22, **2023**, Timisoara, Romania, pp 65.
4. Anca Lascu, **Camelia Epuran**, Ion Fratilescu, Diana Anghel, Eugenia Fagadar-Cosma. Porphyrin-based nanomaterials able to quantify water in food packaging. *The 15<sup>th</sup> Edition of the Conference. "New Trends in Chemistry Research"*, September, 21-22, **2023**, Timisoara, Romania, pp 67.
5. **Epuran Camelia**, Lascu Anca. Acetamide detection with relevance in liver fibrosis control using a dimer compound based on porphyrins. *The 14<sup>th</sup> Edition of symposium with international participation "New trends and strategies in the chemistry of advanced materials with relevance in biological systems, technique and environmental protection "*, 20-21 Octombrie **2022**, Timisoara, Romania, pp 52.
6. Ion Fratilescu, **Camelia Epuran**, Anca Lascu, Mihaela Birdeanu, Eugenia Fagadar-Cosma, Detection of different quinone derivatives using Pt(II)-metalloporphyrin-aunps hybrid nanomaterials. *New Trends and Strategies in the Chemistry of Advanced Materials with Relevance in Biological Systems, Technique and Environmental Protection*, "Coriolan Drăgulescu" Institute of Chemistry, October 20-21, 2022 at Timisoara (Romania).

***VI. Participation and dissemination actions towards the public (scholar, students, interested persons)***

1. The exposition of the poster with the title: Complex between an A<sub>3</sub>B porphyrin, AuNPs and k-carrageenan used for detection of 1-methylimidazole. **Camelia Epuran**, Ion Fratilescu, Diana Anghel, Anca Lascu, Eugenia Fagadar-Cosma: Event: The 19<sup>th</sup> edition of the Night of European Researchers event, funded by the European Commission through Marie Skłodowska-Curie actions, **September 29, 2023**.